Accepted Manuscript

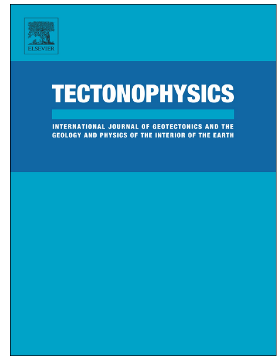

Crustal structure of the SW Iberian passive margin: The westernmost remnant of the Ligurian Tethys?

A. Ramos, O. Fernández, M. Torne, A. Sánchez de la Muela, J.A. Muñoz, P. Terrinha, G. Manatschal, M.C. Salas

PII: S0040-1951(17)30111-7
DOI: doi: 10.1016/j.tecto.2017.03.012
Reference: TECTO 127429

To appear in: *Tectonophysics*

Received date: 11 August 2016
Revised date: 16 March 2017
Accepted date: 20 March 2017

Please cite this article as: A. Ramos, O. Fernández, M. Torne, A. Sánchez de la Muela, J.A. Muñoz, P. Terrinha, G. Manatschal, M.C. Salas , Crustal structure of the SW Iberian passive margin: The westernmost remnant of the Ligurian Tethys?. The address for the corresponding author was captured as affiliation for all authors. Please check if appropriate. Tecto(2017), doi: 10.1016/j.tecto.2017.03.012

Crustal structure of the SW Iberian passive margin: The westernmost remnant of the Ligurian Tethys?

Ramos, A. (1), , Fernández, O. (2), Torne, M. (3), Sánchez de la Muela, A. (4), Muñoz, J.A. (1), Terrinha, P. (5), Manatschal, G. (6), Salas, M.C. (2)

1 Institut de Recerca Geomodels, Departament de Dinàmica de la Terra i de l'Oceà, Universitat de Barcelona, Barcelona, Spain

2 Repsol Exploración, Dirección de Geociencias, Madrid, Spain

3 Institute of Earth Sciences Jaume Almera, ICTJA-CSIC, Spain

4 Department of Geography, University College of London, London, UK. 5 Instituto Português do Mar e da Atmosfera, Divisão de Geologia e Georecursos Marinhos, Lisboa, Portugal

6 Institut Physique du Globe de Strasbourg, Université de Strasbourg - CNRS, Strasbourg, France

Corresponding author.

E-mail address: adria_ramos@outlook.com

Abstract

At present, the SW Iberian margin is located along the convergent Iberia-Nubia plate boundary. In Mesozoic times, the margin was located at the triple junction of the Ligurian Tethys, Central Atlantic and Northern Atlantic. The characterization of its crustal structure has allowed us to propose a configuration for this triple junction and to determine the role that this transform margin played within the plate kinematic system. In this paper we present an integrated study based on the interpretation of a 2D regional multichannel seismic survey consisting of 58 profiles, tied with onshore geology and exploratory wells, and on gravimetric modeling performed over four NW-SE trending profiles.

Integrated interpretation of MCS data combined with 2D gravity modeling reveals a complex pattern in the southward crustal thinning of SW Iberia and supports the possible presence of oceanic crust under the Gulf of Cadiz. The tapering of Iberian crust is characterized by steps with rapid changes in the thickness of the crust, and thinning to less than 10km under the outer portions of the margin. Based on gravimetric modelling results and the structures interpreted on reflection seismic profiles, 3 crustal domains reflecting progressive thinning have been defined for the SW Iberian margin. These domains trend roughly WSW-ENE, parallel to the main extensional fabric of the margin. Gravimetric modeling results are compatible with the presence of exhumed sub-continental mantle in the distal part of the margin. Integrated modeling also supports the fact that Cenozoic contraction is responsible for major uplift along the Guadalquivir Bank. Margin inversion and the pre-existing extensional crustal structure are responsible for the areal distribution and amplitude of the prominent positive gravity anomaly observed in the Gulf of Cadiz.

Keywords: SW Iberian margin, transform margin, margin inversion, crustal structure, gravity, seismic interpretation

1. Introduction

The SW Iberian margin is part of the transform to oblique margin that connected the Ligurian Tethys with the Atlantic (Fig. 1). Left-lateral translation of the Iberian plate during the opening of the Central Atlantic in the Early to Middle Jurassic led to the development of transform margins along southern Iberia and northwestern Nubia. Oceanic crust accreted between Iberia and Nubia during the Mesozoic (Bortolotti and Principi, 2005; Schettino and Turco, 2011) and was later mostly subducted during the emplacement of the Betic-Rif orogen (Gutscher et al., 2012; Schettino and Turco, 2011; Spakman and Wortel, 2004; van Hinsbergen et al., 2014; Vergés and Fernàndez, 2012). This orogen also largely overprinted the former passive margin structure, which is either inverted within the orogen or buried under its thrust system. The only segment of the Iberia-NW Nubia transform margin that has been preserved almost intact to present day is the SW margin of Iberia, running along the northern border of the Gulf of Cadiz (Fig. 1). The existence of highly thinned crust in SW Iberia was initially documented in 1990s along a transect extending from onshore Iberia to the eastern end of the Horseshoe Abyssal Plain (González et al., 1996) (Fig. 1). Based on wide-angle seismic reflection data and gravity modeling, these authors concluded that the crust underwent a strong but continuous thinning from 31 km onshore Iberia to less than 15 km in the Horseshoe Abyssal Plain. Subsequently, a number of geophysical studies have been conducted to investigate the deep structure of the Gulf of Cadiz (Dañobeitia et al., 1999; Gràcia et al., 2003; Gutscher et al., 2002, 2009; Zeyen et al., 2005). The results of these studies show that the crust gently thins from 30-32 km under the Iberian mainland to 25 km in the central part of the Gulf of Cadiz and to 15km in its most western parts. More recently, Sallarès et al. (2011) have published a refraction seismic profile running from the southern Portuguese coast to the deeper western end of the Gulf of Cadiz, which records an abrupt thinning of the continental crust and the transition to oceanic crust occurring in the western Gulf of Cadiz (Fig. 1). Gutscher et al. (2009) and Martínez-Loriente et al. (2014) proposed the prolongation of this oceanic crust to the east under the Gibraltar arc (Fig. 1) (Spakman and Wortel, 2004; van Hinsbergen et al., 2014; Vergés and Fernàndez, 2012).

Fig. 1. a) Location of the study area. Traces of refraction seismic profiles acquired between SW Iberia and NW Africa are from Martínez-Loriente et al. (2014) (P1); González et al. (1996) (P2); Sallarès et al. (2011) (P3); and Contrucci et al. (2004) (P4). The location of the continent-ocean boundary (COB) defined on these lines is shown. The reflection seismic lines interpreted in this work are represented by white lines, while their prolongation to the SE for gravimetric modeling is marked with black dotted lines. AB: Algarve Basin; AUGC: Allochthonous Unit of Gulf of Cadiz; AWGC: Accretionary Wedge of Gulf of Cadiz; GB: Guadalquivir Bank; GoB: Gorringe Bank; HAP: Horseshoe Abyssal Plain; PB: Portimão Bank. SWIM faults come from Zitellini et al. (2009). Bathymetry is taken from the General Bathymetric Chart of Oceans (GEBCO) digital atlas (IOC et al., 2003) and topography from European Environment Agency (EEA). (b) Plate reconstruction at end of Triassic (203 Ma) and (c) at end of Jurassic times (151 Ma) modified after Schettino and Turco (2011), Seton et al. (2012), and Sibuet et al. (2012). 1: NW Nubia, 2: North America, 3: Iberia, 4: Armorica-Greenland.

The nature and origin of the crust under the Gulf of Cadiz is still under dispute. Some authors postulate that the Gulf is floored by Avalonian continental crust north of the Guadalquivir and Portimão Banks (Gràcia et al., 2003; Tortella et al., 1997; Zeyen et al., 2005). According to these authors, the transition to the Atlantic oceanic domain is located to the west and no oceanic crust is interpreted south of the Banks. Alternative interpretations suggest that south of Guadalquivir and Portimão Banks (Fig. 1), there is a corridor of oceanic crust identified on seismic refraction profiles and seismic tomography interpreted as a remnant of the Ligurian Tethys (Gutscher et al., 2002; Martínez-Loriente et al., 2014; Sallarès et al., 2011). Plate kinematic reconstructions that are based on magnetic lineations in the Atlantic (Roeser et al., 2002; Schettino and Turco, 2011; Stampfli and Borel, 2002) suggest a Middle to Late Jurassic age for the first oceanic crust formed along southern Iberia. Nevertheless, the absence of well defined magnetic anomalies in the area has not permitted the dating of this possible oceanic crust or assigning it unambiguously to the Atlantic or Tethyan domains.

Gràcia et al. (2003) and Zeyen et al. (2005) identified the Guadalquivir-Portimão Bank as a feature across which dramatic crustal thinning occurred. This thinning coincides with an ENE-WSW striking gravity anomaly high that extends along the Guadalquivir and Portimão Banks (Fig. 2).The gravity anomaly shows three local highs reaching maximum values above 100 mGal over the Guadalquivir Bank (Fig. 2). This gravity anomaly has been poorly sampled by deep seismic sounding. Reflection profile GC1 (Dañobeitia et al., 1999) was acquired crossing the western part of the anomaly, and refraction profile of Sallarès et al. (2011) was acquired west of the anomaly. As a result, the precise nature of the Gulf of Cadiz gravity anomaly is still under debate.

Fig. 2. Map of free-air gravity anomaly offshore and Bouguer anomaly onshore. Black lines show the location of the 2D gravimetric profiles presented in this study. Note the ENE-WSW trending positive gravity anomaly located offshore (> 40 mGal), and the negative gravity anomaly (<-60 mGal) to the SE. GB: Guadalquivir Bank; PB: Portimão Bank.

The aim of this paper is to provide a geological framework that accounts for the diverse observations made on the crustal structure of the Gulf of Cadiz. The ultimate objective is to understand the crustal structure of the SW Iberian margin and to determine the: 1) the role it played during the Middle to Late Jurassic rifting-drifting stages through to the present-day collisional stage, and 2) its relation to the Nubia-Iberia diffuse plate boundary. In order to achieve these goals we use commercial multichannel seismic reflection (MCS) profiles and published gravity data to construct four profiles that represent the structure of the Gulf of Cadiz.

2. Evolution of the Gulf of Cadiz - Algarve Basin

The Algarve Basin is located along the southern margin of Portugal and extends both onshore and offshore in the Gulf of Cadiz. The evolution of the basin has been documented by many authors; the description contained here is derived from the work of Ramos et al. (2016) and Terrinha (1998) and authors therein, and summarized in Fig. 3.

Rifting in the Algarve Basin initiated in the Triassic, with the generation of isolated half-grabens trending roughly E-W. Triassic siliciclastic continental sediments unconformably overlie Carboniferous flysch deposits belonging to the foreland of the Variscan orogen. Triassic sediments are overlain by earliest Jurassic sediments: Hettangian evaporites and coeval terrigenous clastics, whose distribution is strongly controlled by E-W trending extensional faults. The initial clastic-evaporitic series are capped by a volcanic-sedimentary complex Hettangian-Sinemurian in age that is associated with the Central Atlantic Magmatic Province (CAMP; e.g., Martins et al., 2008). Sinemurian to Toarcian sediments blanket the isolated basins of the first phase of extension and record progressive deepening of the basin. This Early Jurassic subsidence phase ended at the transition to the Middle Jurassic (Terrinha et al., 2002).

Fig. 3. Tectono-sedimentary diagram of the Algarve Basin showing the main stratigraphic units and tectonic events. Modified from Ramos et al. (2016).

Middle Jurassic reactivation of older extensional basins triggered an initial phase of salt tectonism (involving Hettangian evaporites). Extension at this time was dominated by E-W to ENE-WSW trending extensional faults and a NW-SE to NNW-SSE trending relay or transfer zones. Extension and salt tectonism continued through the Middle and Late Jurassic. Middle to Late Jurassic sediments are dominated by carbonates and have highly variable thickness on account of both salt tectonism and extensional faulting. Lower Cretaceous siliciclastics mostly draped over the entire basin and they only locally exhibited variations in thickness related to ongoing salt tectonism or extensional faulting. During the Late Cretaceous sedimentation was very localized and Upper Cretaceous sediments are mostly absent in the basin. The Paleogene is restricted to the offshore as shallow water carbonates. A hiatus at Late Cretaceous-Paleogene times together with an angular unconformity between the Upper Cretaceous and Lower Paleogene successions are evidence of incipient regional uplift during this time.

Sedimentation resumed in the Oligocene with the early pulses of compression between Iberia and Nubia. The base of the Miocene is represented in the Gulf of Cadiz by a regional unconformity (BFU: base foredeep unconformity; Ledesma, 2000). N-S to NW-SE directed shortening during the Neogene led to the partial inversion of the passive margin, with the development of southward directed thrusts that have resulted in a stair-stepped topography and bathymetry (Ramos et al., 2017). During compression, most likely during the Tortonian, the Accretionary Wedge of the Gulf of Cadiz (AWGC; chaotic and mélange-like assemblage of Mesozoic to Cenozoic sediments, Fig. 1) was tectonically emplaced along the entire front of the Betic and Rif into the Atlantic, due to the westward emplacement of the Betic-Rif orogen (Iribarren et al., 2007; Torelli et al., 1997; Gutscher et al., 2002, 2012). The AWGC is partially reworked in the Allochthonous Unit of the Gulf of Cadiz (AUGC; Fig. 1), a gravitationally emplaced submarine debris flows sourced from the AWGC (Iribarren et al., 2007).

3. Data

3.1. Reflection seismic and hydrocarbon exploratory wells

Interpretation of the offshore structure of the Algarve Basin and Gulf of Cadiz is based on a 2D regional seismic survey acquired by TGS in 2001 (PDT00-PD00) and 2D vintage seismic lines property of Repsol covering the proximal Gulf of Cadiz (Fig. 4). The PDT00-PD00 survey consists of 58 lines of 2D multichannel reflection profiles (MCS), striking both NNW-SSW and ENE-WSW. These lines, record down to 12 seconds TWT (two-way time) and were acquired with an streamer length of 6km, and migrated in time (TGS, 2005).

Fig. 4. Data in the Gulf of Cadiz used in this study. The most representative and complete wells shown in this figure are: Alg-1: Algarve-1; Alg-2; Algarve-2; Alm-1: Almonte-1; Asp-1: Asperillo-1; Atl-2-2: Atlantida-2-2; Bet 14-1: Betica 14-1; Bet 18-1: Betica 18-1; Bor-1: Bornos-1; Crv-1: Corvina-1; GC6-X-1; Gulf of Cadiz 6-X-1; GC B-1: Gulf of Cadiz B-1; GC B-2: Gulf of Cadiz B-2; GB D-1: Gulf of Cadiz D-2; GB D-2: Gulf of Cadiz D-2; GB 6Y-1Bis: Gulf of Cadiz 6Y-1Bis; Hue-1: Huelva-1; Imp-1: Imperador-1; Mar-1: Marismas-1; Mog-1: Moguer-1; Ori 2-1: Orion 2-1; Rui-1: Ruivo-1.

The seismic interpretation is tied to onshore geology (Ramos et al., 2016), to 5 wells in the Portuguese offshore (Roque, 2007) and up to 39 wells in the Spanish Gulf of Cadiz area (Lanaja, 1987) (Fig. 4).

Interpretation was performed in Petrel (Schlumberger) taking into account the unconformity bounded sequences defined by Roque (2007) and Terrinha (1998), which were useful to correlate the MCS seismic reflectors through the margin. Seismic sections and their interpretation were converted to depth using Move 2015.1 (by Midland Valley Exploration). Average velocities for three stratigraphic intervals (Neogene-Quaternary, top Paleogene to top Middle Jurassic and top Middle Jurassic to Basement) were derived from the check-shot data from wells Algarve-1, Algarve-2, Corvina-1, Imperador-1 and Ruivo-1 (Fig. 5).

Fig. 5. Checkshot data from the 5 wells in the Portuguese Algarve Basin. See Fig. 4 for location. The time-depth relationships from the 5 wells have been used to define 3 velocity intervals: Neogene-Quaternary (yellow), top Paleogene to top Middle Jurassic (green) and top Middle Jurassic to top of Basement (blue). Data courtesy of Repsol.

Besides formation picks, density values for each stratigraphic unit were derived from the logs available for these 5 wells . Vintage well logs of the Spanish Gulf of Cadiz did not fulfil the quality criteria to be used to obtain density values.

3.2. Gravity

Onshore Bouguer gravity anomalies have been taken from a recent compilation of gravity data on Iberia (Ayala et al., 2016). Offshore, free-air gravity anomalies come from the global satellite altimetry data model V16.1 (Smith and Sandwell, 1997, updated 2007) (Fig. 2). The gravity anomaly in the Gulf of Cadiz is characterized by the presence of an elongated NE-SW gravity high composed by three local highs with values ranging from 40 to 110 mGal. The highest values, above 100 and 80 mGal, coincide with the Guadalquivir and Portimão Banks, respectively (see Fig. 1a). The Guadalquivir Bank is a basement high along which the metamorphosed slates and greywackes of Carboniferous age of the South Portuguese Zone locally crop out at the seafloor (Vegas et al., 2004). The Portimão Bank is a bathymetric high related to an inverted Mesozoic basin (Terrinha et al., 2009). To the north of these Banks, a NE-SW gravity low, with values in a range of -20 to -40 mGal delineates the presence of a large submarine valley that incises the continental slope (Terrinha et al., 2009).The Iberian margin is characterized by positive gravity values (above 20 mGal) that extend from SW Iberia mainland (Fig. 2). As pointed out by Torne et al. (2015), the regional gravity high that delineates the southwestern Variscan terranes of the Ossa Morena and South Portuguese zones is related to the combination of a slight thinning of the crust towards the shoreline and to the presence of a somewhat denser crust relative to the average of the Alpine Iberia (15 to 20 kg/m^3 denser). These results agree with previous seismic studies which found that the mid/lower crust was intruded by a regional high velocity/reflective body and that the base of the crust is located at about 31-32 km (e.g., Carbonell et al., 2004; Palomeras et al., 2009).

By contrast, the central region of the Gulf is characterized by a gravity low (below -100 mGal) that roughly delineates the presence of the low density rocks forming the accretionary wedge (AWGC in Figs. 1a and 2). The wedge thickens towards the east where it reaches thicknesses between 10 km (Thiebot and Gutscher, 2006) and 11.5 km (Iribarren et al., 2007). It consists of a low-density pile of sediments deformed by westward verging imbricate thrust system. Thus the Gulf of Cadiz shows a contrasting duality, the northern segment with predominance of positive free-air gravity anomalies which contrasts with the negative character of its southern areas (Fig. 2). As expected for the offshore free-air gravity anomaly map, short wavelength anomalies correlate to local bathymetry features, but this correlation is not observed for its medium to long-wave length component as this is associated to deeper density lateral variations (see Figs. 1a and 2).

4. Seismic interpretation and gravity modeling

4.1. Seismic interpretation strategy

The interpretation of the offshore structure has been an iterative process involving well-seismic correlation, seismic interpretation and gravity modeling. Interpretation was started from the well locations with wells tied to the time seismic (using the time-depth functions in Fig. 5). Wells offshore Portugal make it possible to constrain horizons down to Middle Jurassic age (Figs. 6 and 7).

Interpretation of seismic profiles has been performed to map the main stratigraphic units defined by Terrinha (1998) (Triassic, Jurassic, Cretaceous and Cenozoic) (Figs. 6, 7 and 8) as well as the main faults, salt diapirs and allochthonous salt bodies (Matias et al., 2011). Each unit has characteristic seismic facies that make it possible to correlate them across faults and salt structures. The Cenozoic is dominated by continuous bright reflectors with multiple wedge and onlap geometries. It can be subdivided internally into the Neogene and Paleogene that are separated by a regional unconformity interpreted to be the base of the Betic foredeep (BFU; Ledesma, 2000). This unconformity, which is easily identified on seismic, corresponds with a strong reflector that truncates underlying units where they are folded or tilted (for instance, in Fig. 6 over the diapir north of well Algrave-1, or south of well Algarve-2).

Along the southern end of some seismic sections (e.g., Figs. 10, 12), the AWGC/AUGC complex is at the same structural position that the Paleogene and Neogene successions. These bodies display internally chaotic or transparent seismic facies. Their top and base are not defined by any characteristic reflectivity but rather by a sharp transition to layered seismic facies above and below (e.g., Fig. 10). Cenozoic sediments deposited above the AWGC/AUGC form mini-basins bounded by shale structures sourced from the allochthonous bodies (e.g., Hernández-Molina et al., 2016; Medialdea et al., 2009). At their base, the AWGC/AUGC can be observed to truncate or be parallel to the underlying Neogene and Paleogene beds (Figs. 12, 13).

The base of the Cenozoic is defined by another, less prominent unconformity. The base Cenozoic unconformity only locally truncates the units below (e.g., south of well Imperador-1 on Fig. 7). Below this unconformity the Cretaceous is characterized by bright and continuous reflectors of lower frequency than the Cenozoic. The Upper Cretaceous is absent in most of the offshore Gulf of Cadiz and the Cenozoic is underlain directly by the Lower Cretaceous. Thickness changes and internal angularities in the Lower Cretaceous related to halokinesis are frequent throughout the area (as in the onshore, Ramos et al., 2016).

Fig. 6. Portion of seismic line 835 across wells Algarve-1 and Algarve-2 in time (a), and seismic interpretation (b). BFU: base foredeep unconformity; K1: Lower Cretaceous; J3: Upper Jurassic; J2:

Middle Jurassic; J1: Upper Jurassic; Tr: Triassic; Ht: Hettangian. The allochthonous Esperança salt unit (Matias et al., 2011) is also identified (Es). See Fig. 4 for location.

The Upper Jurassic lies mostly conformably under the Cretaceous and is dominated by mostly bright but short reflectors of low frequency. The Middle and Lower Jurassic below have a similar seismic facies. Angularities observed within the Jurassic package could correspond to regional unconformities that punctuate rifting of the margin (such as those defined by Terrinha, 1998)and were used to interpret the boundaries between the Lower, Middle and Upper Jurassic. In the proximity of salt diapirs and in some mini-basins, unconformities within the Jurassic are controlled by halokinetic processes. However, major changes in thickness of the Jurassic across basement faults are interpreted to be controlled by extensional faults (for instance, change in thickness across the basement fault on the southern end of Fig. 7, or thickness changes on Figs. 8 and 11).

Fig. 7. Portion of seismic line 816 across the well Imperador-1, in time (a) and seismic interpretation (b). See Fig 4 for location and Fig. 6 for acronyms. Data courtesy of TGS.

The Hettangian evaporite interval, which is deformed into diapirs and salt walls, is the base of the Jurassic succession in the basin. The top and base of the Hettangian evaporites are frequently bright reflectors, and the unit is internally chaotic to transparent. This unit is the deepest unit that is easiest to pick as it is at the base of diapir-related folding and marks the base of halokinetic growth strata. Locally, Hettangian salt is extruded and forms parautochthonous and allochthonous salt bodies (e.g., Matias et al., 2011). Figs. 6 and 8 show one such instance where salt is extruded to form a broad allochthonous salt body (the Esperança Salt) that is emplaced mostly within the Jurassic. Image below this salt body is poor but control on the sub-salt structure is supported by the image in surrounding areas (for instance on Fig. 8). Above the Esperança Salt, mini-basins of Middle Jurassic to Lower Cretaceous developed, with fanning geometries, strong tilting and folding.

Below the Jurassic, the presence of Triassic clastics and volcanics deposited in fault-bounded grabens or half-grabens has been interpreted, by analogy with the onshore (Manuppella, 1992; Ramos et al., 2016; Terrinha, 1998) (for instance, see the half-grabens on the southern end of Fig. 8). The irregular distribution of the Triassic is confirmed by the fact that the only well in the offshore that drilled through the Hettangian evaporites (GC6Y-1BIS, Fig. 4) did not encounter Triassic deposits above the basement. The top of the Triassic unit was mapped on seismic by picking the base of the Hettangian evaporites.

The base of the Triassic has been defined by picking the top of the basement. The position of the top of the basement in the offshore is constrained by well GC6Y-1BIS (Fig. 4) and by its outcrop at the seabed along the Guadalquivir Bank (Vegas et al., 2004). The top of the basement has been interpreted as a bright reflector at the base of fault-bounded growth packages (southern end of Fig. 8). This reflector is sometimes ambiguous on seismic data as the basement is often characterized by reflective facies: its shallower units are Variscan foreland flysch deposits which have limited impedance contrast with the overlying Triassic clastics. The final interpretation of the top of basement has therefore been constrained based on geometric relationships (it is expected to be offset by the same faults as the overlying Mesozoic units).

Fig. 8. Portion of seismic line 826 in the central part of the Algarve Basin, in time (a) and seismic interpretation (b) in the central part of the basin, north of Guadalquivir Bank. Es: Esperança Salt. See Fig 4 for location and Fig. 8 for acronyms. Data courtesy of TGS.

4.2. Main features of the Algarve Basin

Seismic interpretation of the available 2D surveys has made it possible to achieve two key targets. The first one has been to map the basement faults that control the structure of the basin. The most evident faults are the extensional faults that developed during Mesozoic rifting (Figs. 6, 7, 8 and 9a). These faults are observed to trend mostly in a WSW-ENE direction (similar to those on the onshore, Ramos et al., 2016) (Fig. 9a). At the western and eastern ends of the basin, some NW-SE trending faults are observed. Thickness of the Mesozoic is controlled by these faults (Fig. 9a).

Roughly N-S directed compression during the Mesozoic caused the partial inversion of the basin (Ramos et al., 2017) resulting in the present-day configuration of the basement of the basin (Fig. 9b). The faults responsible for inversion are not evident on seismic and have been inferred from multiple criteria, mainly from the tilting and truncation of Mesozoic and Cenozoic units and the geometry of the BFU unconformity (Ramos et al., 2017) (Fig. 10). Despite the inversion of the basin, an overall deepening of the basement towards the south and west is still observed (Fig. 9b), consistent with rifting that generated greater accommodation space in that same direction (Fig. 9a).

Fig. 9. (a) Vertical thickness of Mesozoic (Triassic to Lower Cretaceous) in the SW Iberian margin, with the main Mesozoic extensional faults overlain. Wells on the onshore that encounter Mesozoic sediments are shown in black. Wells that encountered no autochthonous Mesozoic are shown in grey. The Betica 14-1 was finalized upon reaching the top of the autochthonous Mesozoic (Upper Jurassic) and no reliable thickness value can be derived. The Betica 18-1 well drilled 2700m of Mesozoic (Upper and Lower Cretaceous, Jurassic and Triassic). (b) Structural map of the top of basement, affected by Mesozoic extensional faults and Cenozoic thrusts (thrusts from Ramos et al., 2017). Wells reaching the basement are represented in the figure. The Betica 18-1 well encountered the basement at 4280m bsl, but has not been incorporated in the map due to lack of constraint from MCS profiles. See Fig. 4 for complete well names and location of MCS profiles.

The second key target achieved through seismic interpretation was to define the offshore extent of the Algarve Basin. Previous authors have considered the Guadalquivir and Portimão Banks as the southern limit of the Algarve Basin (e.g., Gràcia et al., 2003; Matias et al., 2011; Terrinha et al., 2002). This interpretation was mostly driven by the observed thinning of Mesozoic units onto the Guadalquivir Bank (Figs. 8, 10). Both Banks were interpreted to respond to the same structure. This interpretation has been revised in favor of a combined origin. The Guadalquivir Bank is interpreted as a Mesozoic extensional horst now being carried on top of a southward vergent thrust (Ramos et al., 2017 and Fig. 10). The basement in the Guadalquivir Bank is interpreted to be relatively shallow (less than 2km under the seabed, and locally outcropping) (Malod and Mougenot, 1979; Vegas et al., 2004) and uplifted in the order of 5km in Neogene times due to a major south-directed thrust (Fig. 10). On the other hand, the bathymetric relief of the Portimão Bank is due to the inversion of a Mesozoic extensional half-graben (Ramos et al., 2017; Terrinha et al., 2009 and Fig. 11). As opposed to the Guadalquivir Bank, it is not a basement high, and hence basement depth does not change as dramatically across this feature (Fig. 9b). Thus, the Guadalquivir and Portimão Banks are not considered to be the southern limit of the Algarve Basin.

Fig. 10. Portion of seismic line 828 across the Guadalquivir Bank in time (a) and seismic interpretation (b). The interpretation below 3-4 seconds of TWT is inferred due to the poor deep seismic quality. Interpretation of the northern flank of the Guadalquivir Bank is based on the interpretation performed on 3D seismic (c) of the same structure slightly along strike by (Ramos et al., 2017). See Fig. 4 for location. Data courtesy of TGS.

Fig. 11. Portion of seismic line 805 across the Portimão Bank in time (a) and seismic interpretation (b). The Portimão Bank is imaged as an inverted Mesozoic graben. See Fig 4 for location and Fig. 8 for acronyms. Data courtesy of TGS.

The southern extent of the basin cannot be mapped precisely. However, Mesozoic units are observed to extend south of the Portimão Bank, under the AWGC, possibly over continental basement (Fig. 12). It is further south that oceanic crust can be easily picked on seismic (Fig. 13). The oceanic crust is characterized by a top bright, continuous reflector seen clearly even below the AWGC at roughly 8sec TWT (two-way time). The continent-ocean boundary seen on Fig. 13 is at a location consistent with the continent-ocean boundary documented by Sallarès et al. (2011). Despite the lack of reliable seismic image further to the east, it is interpreted that the southern limit of the Algarve Basin in that direction also lies at the transition to the oceanic crust proposed to be present by Gutscher et al. (2002), Martínez-Loriente et al. (2014), and Sallarès et al. (2011).

Fig. 12. Portion of seismic line 805 south of the Portimão Bank, across a distal portion of the AWGC, in time (a) and seismic interpretation (b). Note that Mesozoic units are visible under the AWGC and the top of the basement is imaged around 7 seconds of TWT. See Fig 4 for location and Fig. 8 for acronyms. Data courtesy of TGS.

Fig. 13. Portion of a seismic profile GM01 across the outer Gulf of Cadiz in time (a) and seismic interpretation (b). Note the bright continuous reflectors under the AWGC interpreted to be the top of oceanic crust. See Fig. 4 for location. Data courtesy of Repsol.

To the east, the Algarve Basin is known to terminate roughly along the present-day coast of SW Spain, where the basement rises (Fig. 9b). Control on the depth of the basement in this area is provided mainly by onshore wells (Fig. 4). Seismic profiles in this area are of limited quality, but some extensional faults have tentatively been mapped to strike NW-SE (Fig. 9a).

The western termination of the Algarve Basin is the only one that has been observed on seismic (Fig. 14). This limit of the basin is characterized by mostly southwestward dipping extensional faults that cause a drastic drop of the basement towards the southwest. The bathymetry in this area is strongly controlled by contouritic currents of the Mediterranean Outflow Water and submarine canyons, but the overall NW-SE trend in the sea bottom runs parallel to the interpreted basement faults. The transition into the oceanic domain on this side of the basin has not been identified on seismic. However, the basement on seismic profiles in this area is interpreted to drop down to 8sec TWT, which is similar to the depth of the top of oceanic crust in Fig. 13 with a similar water column. It is therefore inferred that the continent-ocean boundary does not lie far to the west (or even within the profile).

Fig. 14. Portion of reflection seismic profile 854 across the western portion of the margin (a) and the corresponding interpretation (b). The triangle on the seabed marks the location of the transfer discussed in Fig. 18. See Fig. 4 for location. Data courtesy of TGS.

4.3. Interpreted structure

To represent the structure of the Gulf of Cadiz, four cross-sections have been interpreted following key seismic profiles (Fig. 15). These sections strike NNW-SSE, with the objective of intersecting the southern limit of the Algarve Basin and the prominent positive gravity anomaly that runs along the Guadalquivir and Portimão Banks (Fig. 2). Interpretation on these sections was driven by seismic (e.g., Figs. 6 through 11) for the shallower Algarve Basin (the area north of the Guadalquivir and Portimão Banks).

The structure of the shallow Algarve Basin is characterized by both south and north dipping extensional faults, with growth from Triassic to Middle Jurassic (Fig. 15). Throw on the faults and thickness of Jurassic depocenters increases progressively southwards (Figs. 9a and 15). Thickness changes in the Jurassic are partly controlled by salt tectonics (e.g., mini-basin south of Imperador-1 in Fig. 7) and partly fault-driven (e.g., Mesozoic half-graben in Fig. 11). In the case of the Lower Cretaceous and Paleogene, thickness changes are largely controlled by salt withdrawal in mini-basins (e.g., depocenters flanking the structure near well Algarve-1 on Fig. 6) and by erosion during uplift (e.g., over diapir south of well Imperador-1 on Fig. 7).

To the south of these Banks, image quality makes it difficult to define the structure unambiguously. Initial gravity modeling of key sections in the area (Giraldo et al., 2014; Ramos et al., 2015) demonstrated that the basement on the southern side of the Guadalquivir-Portimão Bank lies 5-7km deeper than under the Algarve Basin, indicating that the crust needs to be significantly thinner. Thinning of the crust is consistent with the interpreted drop in the top of the basement and southward increase in Mesozoic accommodation space (Fig. 9). . However, greater thickness of Miocene-Present sediments and the presence of the AWGC and AUGC south of the Guadalquivir-Portimão Bank pose major challenges to correlate Mesozoic horizons from the Algarve Basin into deeper water areas. Interpretation to the south of the Guadalquivir and Portimão Banks was therefore focused on identifying the base of the AWGC/AUGC and the most likely top of basement (e.g., Figs. 10 and 12).

Fig. 15. Interpretation of depth converted seismic profiles through the Algarve Basin, shown from west (top) to east (bottom): a) Line 805; b) Line 816; c) Line 826; and d) Line 835. The control points on the depth of Moho from the compilation of Diaz et al. (2016) and the profile of Sallarès et al. (2011) are shown. Average interval densities are shown in the legend. GB: Guadalquivir Bank; PB: Portimão Bank. See Figs. 1a and 4 for location. Data courtesy of TGS.

4.4. Gravity modeling

The four representative cross-sections presented in Fig. 15 were modeled for their gravimetric response with three objectives: 1) to validate the interpreted depth to basement, particularly relevant in areas of poor seismic imaging; 2) to constrain the structure to the south of the Guadalquivir-Portimão Bank, where the AUGC/AWGC obscures the deep structure; and 3) to characterize the crustal structure of the passive margin by combining gravity with available well log data to constraint densities at upper crustal levels and available seismic wide angle and refraction data to constraint the depth to the base of the crust and the densities at mid-lower crustal and uppermost lithospheric mantle levels. For the sedimentary cover and geometry of top of basement, the gravity models shown in Fig. 16 were built using the geometry derived from the seismic interpretation discussed above (Fig. 15) and well log data. For the deeper part of the profiles, from top basement to the base of the crust we have used information from all available wide-angle and refraction seismic data, and previous 2D crustal and lithosphere geophysical modeling (Fernàndez et al., 2004; González et al., 1998; Gutscher et al., 2002; Zeyen et al., 2005). Along the Iberia continental margin, Moho depths were taken from the compilation of Diaz et al. (2016) and the profiles of Palomeras et al. (2009). For the distal parts of the profiles we have taken the data from Gutscher et al. (2012). For the continental domain of the westernmost profiles Moho depths were taken from Sallarès et al. (2011). Well logs were mainly used to constrain the density of the main sedimentary units whilst the density of the crystalline crust were converted from P-wave velocities to densities by using the Brocher (2005) empirical relationship. . The crust is modelled as: sedimentary layers with densities that range from 2200 to 2600 kg/m^3, an underlying upper/middle crust with an average density of 2750 kg/m^3, while for the lower crust and uppermost lithospheric mantle we have used 2900 and 3300 kg/m^3, respectively. The forward modeling has been performed using GM-SYS (modeling application of Oasis Montaj, Geosoft software), which calculates the gravity response of the density models built using the methods of (Talwani, 1965; Talwani et al., 1959). For all transects (Figs. 16 and 17) the calculated gravity values lie very close to measurements.

5. Results: Crustal structure of the SW Iberian margin

The results of the modeling process are 4 profiles (Figs. 16 and 17) that capture the key aspects of the SW Iberian passive margin. These profiles follow the seismic lines shown in Fig. 15, and are extended towards the south, into the region of the negative free-air gravity anomaly (Fig. 2).

Fig. 16. Composition of observed and forward modelled gravity, density model and final interpretation for profiles along lines 805 (a) and 816 (b). The geometry of the sedimentary layers, from Triassic to Quaternary, has been derived from the interpretation of MCS data (Fig. 15). Extent of the seismic profiles is represented by a black box on the density model. Densities used are also shown in the table on Fig. 15. The Moho from the profile of Sallarès et al. (2011) has been projected onto the density models over the pertinent segments. Points from the compilation by Diaz et al. (2016) lying on the modelled profiles (black) and projected from nearby locations (white) are also shown on the density model. On the final interpretation note the combination of Mesozoic extensional and Cenozoic contractional features (from Ramos et al., 2017). See text for a discussion of the defined crustal domains. PB: Portimão Bank. See Fig. 2 for location.

Modeling results demonstrate that the originally interpreted top of basement is regionally valid. Locally, however, gravimetric modeling reveals that depocenters under the Hettangian evaporites are thicker than initially interpreted. Results have therefore been used to fine tune the interpretation in these sectors (revised interpretation shown in Figs. 16 and 17). The final interpreted thickness of some of these Triassic depocenters is much greater than that observed onshore (few hundreds of meters, Ramos et al., 2016) but in line with thicknesses observed in basins such as the High Atlas or Essaouira (Domènech et al., 2015; Ellouz et al., 2003; Le Roy and Piqué, 2001).

At the crustal scale, gravimetric modeling supports the interpretation of thinning of the crust towards the axial parts of the Gulf of Cadiz. The transition from the thick crust along the northern end of the profiles to the thin crust along the southern end of the profiles is interpreted as defining four key domains. The northernmost domain (proximal domain, Figs. 16 and 17) is characterized by a limited amount of thinning (the pre-rifting crust is 20-26km thick, equivalent to β between 1.25 and 1.6). This proximal domain has approximately constant crustal thickness, water depth and depth to basement. From this domain to the south the first increase in the gravity signal occurs above the point where the crust starts to thin significantly along with an increase in water depth. Thinning is gradual in the eastern profiles (lines 826, 835, Fig. 17). In the west, crustal thinning concentrates across one or two relatively narrow steps, 10 to 15km wide (lines 805, 816, Fig. 16). The domain of thinning (necking domain) is wider in the west (in the order of 75km, line 805, Fig. 16) and becomes narrower towards the east (less than 50km wide, line 835, Fig. 17).

Gravimetric modeling also suggests that the most pronounced thinning of the continental crust occurs at the southern end of the necking domain, just underneath the gravity high. At this location, the Moho is modelled to be only 15km deep and the crust 10km thick or less (Figs. 16, 17). The crust in this area is known to be continental. Carboniferous basement rocks have been dredged from the Guadalquivir Bank (Vegas et al., 2004) and the Portimão Bank is a Mesozoic graben that must have developed over continental crust.

South of the necking domain we have interpreted the presence of a domain of highly attenuated continental crust (distal domain). Continental crust in the distal domain has been interpreted to be faulted and rotated by low-angle extensional faults (Figs. 16, 17). This interpretation is partly based on observations made on seismic data, such as the folded geometry of Mesozoic strata south of the Portimão Bank (Fig. 12) or the local presence of diapirs rising from the deep Mesozoic strata south of the Guadalquivir Bank (our interpretation in Fig. 10 and Medialdea et al., 2004).

We have assumed that serpentinized mantle could be present in the distal domain by exhumation of the uppermost lithospheric mantle during Jurassic extension. The gravity contribution of serpentinized mantle bodies is in the range of 20 to 30 mGal. Although we do not have any direct evidence for the presence of Jurassic exhumed mantle in the study region, we have assumed its presence by affinity with what is observed in the West Iberian Atlantic Margin (e.g., Peron-Pinvidic and Manatschal, 2009). Serpentinized sub-continental mantle exhumed in the Late Jurassic to Early Cretaceous has also been documented in neighboring areas such as the Gorringe Bank (Cornen et al., 1999; Jimenez-Munt et al., 2010) or the Rif (Michard et al., 2007).

Fig. 17. Composition of observed and forward modelled gravity, density model and final interpretation for profiles along lines 826 (a) and 835 (b). The geometry of the sedimentary layers, from Triassic to Quaternary, has been derived from the interpretation of MCS data (Fig. 15). Extent of the seismic profiles is represented by a black box on the density model. Densities used are also shown in the table on Fig. 15. The Moho control points from Diaz et al. (2016) are shown on the density model. On the final interpretation note the combination of Mesozoic extensional and Cenozoic contractional features (from Ramos et al., 2017). The geometry on the southern end of the profiles is partly inferred from that seen on the western profiles (Fig. 16). See text for a discussion of the defined crustal domains. GB: Guadalquivir Bank. See Fig. 2 for location.

In the longer profiles (Fig. 16), a thin high density crust has been interpreted in the southernmost part. This crust has been interpreted as a possible oceanic crust (density of 2900kg/m^3), driven by the observations on reflection seismic in this area (Fig. 13) and by the work of previous authors (e.g., Gutscher et al., 2009; Martínez-Loriente et al., 2014; Sallarès et al., 2011).

The effect of Cenozoic inversion of the SW Iberian margin is also observed on the modeled profiles. Inversion in this margin has localized mainly in the necking and distal domains. In the west the necking domain is broad and the transition to the distal domain is gradual and located south of the Portimão Bank (Fig. 16a). In this sector, Cenozoic contraction caused the inversion of pre-existing rift structures, but did not cause major uplift of the basement. Towards the east the necking domain becomes narrower and the transition to the distal and oceanic domains becomes very sharp (Fig. 17b). This transition is located immediately south of the Guadalquivir Bank. To account for this geometry, we interpret that the extensional structure of the southern flank of the Guadalquivir Bank was originally similar to that south of the Portimão Bank. Cenozoic inversion in the Guadalquivir Bank subsequently occurred along crustal-scale thrusts that caused major uplift along the Bank and folded and tilted the pre-existing extensional structure into its present-day geometry.

According to our preferred interpretation, the width of the necking and distal domains accounts for the varying wavelength of the positive gravity anomaly of the Gulf of Cadiz. In the case of Portimão Bank (Fig. 16a) the anomaly is broad due to the greater width of the necking domain and is not related to a basement high (the top of the basement is in the order of 8km deep; Figs. 11 and 15a). On the other hand, crustal thinning further east (Fig. 17b) is more abrupt on account of the superposition of the initial extensional geometry and subsequent basement uplift (Guadalquivir Bank: Ramos et al., 2017; Vegas et al., 2004),. This explains the narrower and stronger positive anomaly.

6. Discussion

The present-day crustal structure of the SW Iberian margin is the result of the superposition of Mesozoic extension and Cenozoic to Present shortening. The discussion below will first describe the more recent contractional overprint before discussing the original crustal structure related to extension.

6.1. Inversion of the SW Iberian margin

The effects of Cenozoic shortening are most evident in the eastern part of the Algarve Basin, in particular along the Guadalquivir Bank (Figs. 10 and 17). In this eastern part of the basin, the Guadalquivir Bank is uplifted by at least 2km due to Cenozoic basement-involving thrusting (Ramos et al., 2017). To the west, the Portimão Bank is observed to be mildly inverted with no evidence of significant thrusting in the basement (Fig. 11; Ramos et al., 2017). This difference in the magnitude of Cenozoic shortening accounts for the differences in the geometry of the transition from the necking to the distal domains. In the west, the necking domain is broad and it transitions gradually into the distal domain. The result is a broad high in the Moho (Figs. 16 and 18a). In the east, this structure has been strongly overprinted by contraction and uplift, resulting in what appears as a narrow antiformal geometry of the Moho (Fig. 17). The geometry of the distal domain is also interpreted to be highly affected by uplift and tilting due to contraction (Figs. 17). The contractional overprint leads to the shallow in the base of the crust becoming much narrower and offset further southeast in the eastern sections (Fig. 18a). The offset observed in the base of the crust coincides with the trace of a NW-SE trending thrust identified by Ramos et al. (2017)that also causes a major step in the map trace of the necking zone (Fig. 18b), supporting the crustal nature of these thrusts.

The main inversion structure in the Gulf of Cadiz coincides in location and strike with the necking zone along the Guadalquivir Bank (Figs. 17, 18b). This raises the possibility that the thrust under the Guadalquivir Bank takes advantage of the tilting of the lower crust and Moho induced initially during extensional necking (Fig. 17). The localization of inversion along the necking zone contrasts with the inversion documented by Tugend et al. (2014) along northern Iberia and Druet (2016) along northwest Iberia, where thrusting is located in the distal domain or the continent-ocean transition. The possibility of similar structures in the deep part of the modelled profiles cannot be ruled out but they cannot be identified due to the masking by the AWGC/AUGC.

Inversion of the Guadalquivir Bank can help explain the apparent lack of isostatic equilibrium of the structure based on the interpreted crustal structure. Based on the water column (less than 1km) and relatively shallow depth to basement (less than 1km below seabed) in the Guadalquivir Bank on line 826 (Fig. 15c), the Moho would be expected to be in the order of 28km deep (by comparison with the onshore Iberian Moho at 32km depth and assuming a 2800kg/m^3 average crustal density and Airy isostasy). This value is significantly deeper than estimates from DSS (Diaz et al., 2016) and our model (Fig. 17a) that place it at 24 or 15km depth respectively. This contrasts with the Portimão Bank where under roughly 2km of water and 8km of sediments, the Moho is expected at 18km depth, in line with our model (Fig. 16a). The relevance of flexure in supporting isostatic disequilibrium cannot be ignored. Flexure of the lithosphere west of the Gibraltar Arc subduction could be responsible for the broad negative anomaly observed south of the lines 826 and 835 (Fig. 2).

Fig. 18. a) Map of the base of the crust derived from seismic interpretation and gravimetric modeling. The COT (continent-ocean transition) derived from gravimetric modeling is shown by the bold dashed line. Points with numbers indicate the depth to the base of the crust from the compilation of Diaz et al. (2016). The western limit of the Gulf of Cadiz (GoC) segment of the margin is marked by the Gorringe-GoC transfer zone along the transition from continental to ocean domains defined by González et al., (1996) and Sallarès et al. (2011). The eastern limit of the margin segment is located along the GoC-Betic transfer zone, across which Mesozoic thickness drops (dashed contours indicate Mesozoic thickness in this area from the map in Fig. 9a). b) Map of crustal thickness of SW Iberia with crustal domains (proximal, necking, and distal) defined through gravimetric modeling and from crustal thickness. Thrusts relevant to the discussion, mapped by Ramos et al. (2017), and relevant extensional faults from Fig. 9a are superimposed.

6.2. Extensional crustal structure of SW Iberia

What remains at crustal level after discounting the effects of Cenozoic contraction is a gross southeastward directed thinning of the SW Iberian margin (Fig. 18b). Southeastward thinning is the result of extension in the Mesozoic, which was dominated by WSW-ENE to E-W faulting, with NW-SE trending transfer faults (Fig. 9b; trends also in the onshore: Ramos et al., 2016).

The orientation of the crustal domains resulting from thinning in the westernmost Algarve Basin rotates to a southwestward direction (Fig. 18b). This western margin of the basin coincides with a sharp rise in the Moho that trends NW-SE (Fig. 18a), parallel to the transfer faults of the extensional system. It is therefore proposed that southeastward thinning is due to margin-perpendicular extension, whereas crustal thinning across the western end of the margin occurs across transfer faults (e.g., Fig. 14).

This proposed orientation of the margin accounts for the main difference between our models and the interpretation of Sallarès et al. (2011). These authors interpret continental crust to transition directly to oceanic crust at the point where crust thins to less than 10km immediately south of the Portimão Bank. This rapid transition contrasts with the more gradual transition suggested by our modeling (Fig. 16). The difference arises because the continent-ocean transition in the profile of Sallarès et al. (2011) occurs across the transform system bounding the Algarve Basin to the west (Fig. 18a). On the other hand, the transects presented in this paper are drawn perpendicular to the dominant extensional faults and therefore provide an image of the transition from continental to oceanic crust in the direction of extension.

The orientation of this margin is consistent with that expected from the relative motion between Iberia and NW Nubia during the Jurassic (Figs. 1b and 1c; Schettino and Turco, 2011). This trend is noticeably different to the N-S to NE-SW trend of the Atlantic margins (Fig. 1) and makes the SW Iberian passive margin the likely westward continuation of the southern Iberian passive margin (currently inverted in the Betics) and possibly the Ligurian Tethys.

Oceanization in southern Iberia is understood to have occurred during the Late Jurassic (García-Hernández et al., 1989; Vera et al., 2004), an age similar to the age of ophiolites of the Ligurian Tethys (Bortolotti and Principi, 2005). In this context, it is possible that the thin, relatively high density crust interpreted at the southern end of the 4 profiles (Figs. 16 and 17) is actually Late Jurassic oceanic crust.

The prominent ENE-WSW trending positive gravity anomaly of the Gulf of Cadiz is therefore interpreted to represent the locus of extreme crustal thinning and the presence of high density bodies (serpentinized mantle) in the transition from continental to oceanic crust, as observed further north in the Iberian Atlantic and Cantabrian margins (Peron-Pinvidic and Manatschal, 2009; Tugend et al., 2014). It is interpreted that the rise in the mantle is locally driven by thinning of the lower crust (Figs. 17a,b), indicating heterogeneous thinning of the crust during rifting. The width of the necking domain and the Cenozoic inversion are the factors that control the width and amplitude of the positive anomaly.

6.3. Regional context

The continent-ocean transition proposed from gravimetric modeling (Fig. 17) trends roughly WSW-ENE (Fig. 18b), consistent with the regional trend of the margin. It provides a better estimate of the northern limit of oceanic crust in the Gulf of Cadiz than those proposed to date (e.g., Gutscher et al., 2009; Martínez-Loriente et al., 2014).

The lateral continuity of the passive margin as mapped in Fig. 18b is limited to both east and west. To the east, interpretation of vintage seismic and well data that shows a rapid eastward rise in the basement and decrease in Mesozoic thickness just east of the present-day coastline (Fig. 9). The basement remains relatively shallow and the Mesozoic is absent under the foreland Guadalquivir Basin (Lanaja, 1987). This transition is interpreted to occur across a NW-SE zone of transfer (already proposed by Lanaja, 1987) dominated by NW-SE striking extensional or transtensional faults, labelled Gulf of Cadiz-Betics transfer zone in Fig. 18a.

To the west, a similar transition is inferred where the Moho becomes shallow, west of the Portimão Bank (Fig. 18a). This transition is observed to be controlled by westward dipping extensional faults (Figs. 9, 14) that drop the top of basement to depths similar (10-12km) with that of the oceanic crust interpreted in the Horseshoe Abyssal Plain by Martínez-Loriente et al. (2014). The faults identified along the western Algarve Basin coincide in location (see triangle on the seabed in Fig. 14) with a sudden rise in the Moho that trends NW-SE (based on the profiles of González et al., 1996 and Sallarès et al., 2011; Fig. 18a). This is interpreted to represent another NW-SE trending transfer zone that in this case may link the site of Mesozoic mantle exhumation of the Gorringe Bank with the proposed exhumed mantle of the Portimão Bank (Gorringe-Gulf of Cadiz transfer, Fig. 19).

The SW Iberian passive margin in the Gulf of Cadiz is therefore interpreted to correspond to a segment of the transform margin that connected the Central Atlantic and the Ligurian Tethys during the Jurassic and Cretaceous. Assuming oceanization of this margin occurred in the Late Jurassic (Bortolotti and Principi, 2005; García-Hernández et al., 1989; Vera et al., 2004), oceanic crust would have formed as part of the Iberia-Africa conjugate (Fig. 1c), at the westernmost end of the Ligurian Tethys.

To the south, the contact with the Nubia plate is not identifiable in our models due to their limited length. Nonetheless, the SWIM lineaments (Zitellini et al., 2009) continue to be a good candidate for the location for this boundary. The SWIM lineaments coincide with the location of a roughly E-W trending boundary in the free-air gravity anomaly (Fig. 19) which may reflect the boundary between both plates. In the eastern portion this boundary is between Nubia continental crust and possibly Tethyan oceanic crust. In the center and to the west, the boundary juxtaposes oceanic crust on both sides (Fig. 19). The nature of the crust south of the Gorringe Bank is not certain but has been proposed by Martínez-Loriente et al. (2014) to be Tethyan.

Fig. 19. a) Map of the main crustal domains of the Gulf of Cadiz and surrounding areas. Bathymetry is shown in the background (contours every 200m). The location of bibliographic profiles is shown. The domains defined for the Morocco margin are derived by projecting the domains defined by Contrucci et al. (2004). b) Map of the free-air gravity anomaly map (offshore) and Bouguer gravity anomaly (onshore) of the SW Iberian margin with the crustal domain distribution based on integrated regional 2D seismic data and gravimetric modeling. Thin dashed black lines: crustal domain boundaries.

7. Conclusions

Integrated seismic interpretation and gravimetric modeling have made it possible to propose a crustal structure in a regional context for the SW Iberian margin. The crustal structure of the SW Iberian margin is observed to result from the superposition of Mesozoic extension and Cenozoic inversion of the margin. The result of Mesozoic extension was a southward thinning of the SW Iberian margin. This structure is best preserved in the western Gulf of Cadiz where the effects of Cenozoic inversion are less strong, and indicates that crustal thinning occurs in a stepped manner across a zone nearly 100km wide.

The SW Iberian margin is interpreted to correspond to the westernmost segment of the Ligurian Tethys. In this context, the Gulf of Cadiz represents a segment of the margin comprised between the Betic margin in the east and a possibly Atlantic domain to the west.

The large positive gravity anomaly of the Gulf of Cadiz corresponds to the zone of greatest crustal attenuation, where the continental crust is interpreted to be as thin as 10km or less. Cenozoic inversion in the eastern Gulf of Cadiz concentrated in this domain of thin continental crust, causing folding at crustal level. The result is a larger amplitude and narrower gravity anomaly.

Acknowledgements

This study was funded by Repsol Exploración (Madrid) and partially supported by the SALTECRES project (CGL2014-54118-C2-1-R MINECO/FERDER, UE). A. Ramos' PhD research is funded by Repsol Exploración. The authors wish to thank L. Cascone, A. Olaiz, W. Hermoza, R. Rocca and C.

Giraldo preceded our work on the structure of the south Portuguese margin and set us on the right track. We also are grateful to A. Arnaiz and the Iberia Exploration Team at Repsol for continued support and enriching discussions. The authors also wish to thank four anonymous reviewers for the discussion that have greatly helped us improve this paper. We also acknowledge Schlumberger, Midland Valley and Oasis Montaj for the academic software licenses used for seismic interpretation, cross-section construction and gravity modeling respectively. Fig. 2 and the background maps of Fig. 19 have been made using GMT academic software (Wessel and Smith, 1998). Repsol and Partex-Oil&Gas provided us their proprietary vintage seismic surveys and a 3D seismic cube, published with their permission. Seismic lines of the PDT00-PD00 survey have been provided by TGS and published with the permission of TGS. The seismic PDT00-PD00 survey is available for purchase from TGS and ENMC (Entidade Nacional para o Mercado de Combustibles).

References

Ayala, C., Bohoyo, F., Maestro, A., Reguera, M.I., Torne, M., Rubio, F., Fernàndez, M., García-Lobón, J.L., 2016. Updated Bouguer anomalies of the Iberian Peninsula: a new perspective to interpret the regional geology. J. Maps 1–4. doi:10.1080/17445647.2015.1126538

Bortolotti, V., Principi, G., 2005. Tethyan ophiolites and Pangea break-up. Isl. Arc 14, 442–470. doi:10.1111/j.1440-1738.2005.00478.x

Brocher, T.M., 2005. Empirical Relations between Elastic Wavespeeds and Density in the Earth's Crust. Bull. Seismol. Soc. Am. 95, 2081–2092. doi:10.1785/0120050077

Carbonell, R., Simancas, F., Juhlin, C., Pous, J., Pérez-Estaún, A., Gonzalez-Lodeiro, F., Muñoz, G., Heise, W., Ayarza, P., 2004. Geophysical evidence of a mantle derived intrusion in SW Iberia. Geophys. Res. Lett. 31, n/a-n/a. doi:10.1029/2004GL019684

Contrucci, I., Klingelhöfer, F., Perrot, J., Bartolome, R., Gutscher, M.-A., Sahabi, M., Malod, J., Rehault, J.-P., 2004. The crustal structure of the NW Moroccan continental margin from wide-angle and reflection seismic data. Geophys. J. Int. 159, 117–128. doi:10.1111/j.1365-246X.2004.02391.x

Cornen, G., Girardeau, J., Monnier, C., 1999. Basalts, underplated gabbros and pyroxenites record the rifting process of the West Iberian margin. Mineral. Petrol. 67, 111–142. doi:10.1007/BF01161518

Dañobeitia, J.J., Bartolomé, R., Checa, A., Maldonado, A., Slootweg, A.P., 1999. An interpretation of a prominent magnetic anomaly near the boundary between the Eurasian and African plates (Gulf of Cadiz, SW margin of Iberia). Mar. Geol. 155, 45–62. doi:10.1016/S0025-3227(98)00140-6

Diaz, J., Gallart, J., Carbonell, R., 2016. Moho topography beneath the Iberian-Western Mediterranean region mapped from controlled-source and natural seismicity surveys. Tectonophysics. doi:10.1016/j.tecto.2016.08.023

Domènech, M., Teixell, A., Babault, J., Arboleya, M.-L., 2015. The inverted Triassic rift of the Marrakech High Atlas: A reappraisal of basin geometries and faulting histories. Tectonophysics 663, 177–191. doi:10.1016/j.tecto.2015.03.017

Druet, M., 2016. Geodinámica del margen continental de Galicia: estructura profunda y morfotectónica. PhD Thesis, 251 pp. Universidad Complutense de Madrid, Madrid.

Ellouz, N., Patriat, M., Gaulier, J.-M., Bouatmani, R., Sabounji, S., 2003. From rifting to Alpine inversion: Mesozoic and Cenozoic subsidence history of some Moroccan basins. Sediment. Geol., Integrated Peri-Tethyan Basins Studies (Peri-Tethys Programme) 156, 185–212. doi:10.1016/S0037-0738(02)00288-9

Fernàndez, M., Marzán, I., Torne, M., 2004. Lithospheric transition from the Variscan Iberian Massif to the Jurassic oceanic crust of the Central Atlantic. Tectonophysics 386, 97–115. doi:10.1016/j.tecto.2004.05.005

García-Hernández, M., López-Garrido, Á.C., Martín-Algarra, A., Cámara, J.M., Ruiz-Ortiz, P.A., Vera, J.A., 1989. Las discontinuidades mayores del Jurásico de las Zonas Externas de las Cordilleras Béticas: análisis e interpretación de los ciclos sedimentarios. J. Iber. Geol. 35–52.

Giraldo, C., Hermoza, W., Amigo, B., Rocca, R., Martínez, C., Malmcrona, Y., Rosales, C., Baudino, R., Martín-Monge, A., Fernández, O., Welsink, H., Cascone, L., Olaiz, A., García-Mojonero, C., Arnaiz, A., 2014. Evidences of Salt Tectonics around the Guadalquivir bank, Gulf of Cádiz (SW Iberia). Presented at the AAPG 2014 European Regional Conference & Exhibition, Barcelona, Spain, May 13-15, 2014. Search and Discovery Article #50980.

González, A., Córdoba Barba, D., Vegas, R., Matías, L.M., González Fernández, A., Córdoba Barba, D., Vegas, R., Matías, L.M., 1998. Seismic crustal structure in the southwest of the Iberian Peninsula and the Gulf of Cadiz. Tectonophysics 296, 317–331.

González, A., Torne, M., Córdoba, D., Vidal, N., Matias, L.M., Díaz, J., 1996. Crustal thinning in the Southwestern Iberia Margin. Geophys. Res. Lett. 23, 2477–2480. doi:10.1029/96GL02299

Gràcia, E., Dañobeitia, J., Vergés, J., Bartolomé, R., Córdoba, D., 2003. Crustal architecture and tectonic evolution of the Gulf of Cadiz (SW Iberian margin) at the convergence of the Eurasian and African plates. Tectonics 22, 1033. doi:10.1029/2001TC901045

Gutscher, M.-A., Dominguez, S., Westbrook, G.K., Le Roy, P., Rosas, F., Duarte, J.C., Terrinha, P., Miranda, J.M., Graindorge, D., Gailler, A., Sallares, V., Bartolome, R., 2012. The Gibraltar subduction: A decade of new geophysical data. Tectonophysics 574–575, 72–91. doi:10.1016/j.tecto.2012.08.038

Gutscher, M.-A., Dominguez, S., Westbrook, G.K., Leroy, P., 2009. Deep structure, recent deformation and analog modeling of the Gulf of Cadiz accretionary wedge: Implications for the 1755 Lisbon earthquake. Tectonophysics 475, 85–97. doi:10.1016/j.tecto.2008.11.031

Gutscher, M.-A., Malod, J., Rehault, J.-P., Contrucci, I., Klingelhoefer, F., Mendes-Victor, L., Spakman, W., 2002. Evidence for active subduction beneath

Gibraltar. Geology 30, 1071. doi:10.1130/0091-7613(2002)030<1071:EFASBG>2.0.CO;2
Hernández-Molina, F.J., Sierro, F.J., Llave, E., Roque, C., Stow, D.A.V., Williams, T., Lofi, J., Van der Schee, M., Arnáiz, A., Ledesma, S., Rosales, C., Rodríguez-Tovar, F.J., Pardo-Igúzquiza, E., Brackenridge, R.E., 2016. Evolution of the gulf of Cadiz margin and southwest Portugal contourite depositional system: Tectonic, sedimentary and paleoceanographic implications from IODP expedition 339. Mar. Geol. 377, 7–39. doi:10.1016/j.margeo.2015.09.013
IOC, IHO, BODC, 2003. Centenary Edition of the GEBCO Digital Atlas, published on CDROM on behalf of the Intergovernmental Oceanographic Commission and the International Hydrographic Organization as part of the General Bathymetric Chart of the Oceans, British Oceanographic Data Centre, Liverpool, UK.
Iribarren, L., Vergés, J., Camurri, F., Fullea, J., Fernàndez, M., 2007. The structure of the Atlantic–Mediterranean transition zone from the Alboran Sea to the Horseshoe Abyssal Plain (Iberia–Africa plate boundary). Mar. Geol. 243, 97–119. doi:10.1016/j.margeo.2007.05.011
Lanaja, J.M., 1987. Contribución de la exploración petrolífera al conocimiento de la geología de España. IGME, Madrid.
Le Roy, P., Piqué, A., 2001. Triassic–Liassic Western Moroccan synrift basins in relation to the Central Atlantic opening. Mar. Geol. 172, 359–381. doi:10.1016/S0025-3227(00)00130-4
Ledesma, S.M., 2000. Astrobiocronología y estratigrafía de alta resolución del Neógeno de la Cuenca del Guadalquivir-Golfo de Cádiz. PhD Thesis, 464 pp. Universidad de Salamanca.
Malod, J.A., Mougenot, D., 1979. L'histoire geologique neogene du golfe de Cadix. Bull. Soc. Geol. Fr. S7–XXI, 603–611. doi:10.2113/gssgfbull.S7-XXI.5.603
Manuppella, G., 1992. Carta geológica da região do Algarve. Noticia explicativa da Carta Geologica da regiao do Algarve. Serviços geológicos de Portugal.
Martínez-Loriente, S., Sallarès, V., Gràcia, E., Bartolome, R., Dañobeitia, J.J., Zitellini, N., 2014. Seismic and gravity constraints on the nature of the basement in the Africa-Eurasia plate boundary: New insights for the geodynamic evolution of the SW Iberian margin: Thin oceanic crust at the CPR and SH. J. Geophys. Res. Solid Earth 119, 127–149. doi:10.1002/2013JB010476
Martins, L.T., Madeira, J., Youbi, N., Munhá, J., Mata, J., Kerrich, R., 2008. Rift-related magmatism of the Central Atlantic magmatic province in Algarve, Southern Portugal. Lithos 101, 102–124. doi:10.1016/j.lithos.2007.07.010
Matias, H., Kress, P., Terrinha, P., Mohriak, W., Menezes, P.T.L., Matias, L., Santos, F., Sandnes, F., 2011. Salt tectonics in the western Gulf of Cadiz, southwest Iberia. AAPG Bull. 95, 1667–1698. doi:10.1306/01271110032
Medialdea, T., Somoza, L., Pinheiro, L.M., Fernández-Puga, M.C., Vázquez, J.T., León, R., Ivanov, M.K., Magalhaes, V., Díaz-del-Río, V., Vegas, R., 2009. Tectonics and mud volcano development in the Gulf of Cádiz. Mar. Geol., EUROMARGINS: Imaging, monitoring, and modelling the physical, chemical and biological processes in the European passive continental margins 261, 48–63. doi:10.1016/j.margeo.2008.10.007
Medialdea, T., Vegas, R., Somoza, L., Vázquez, J.T., Maldonado, A., Díaz-del-Río, V., Maestro, A., Córdoba, D., Fernández-Puga, M.C., 2004. Structure and evolution of the "Olistostrome" complex of the Gibraltar Arc in the Gulf of Cádiz (eastern

Central Atlantic): evidence from two long seismic cross-sections. Mar. Geol. 209, 173–198. doi:10.1016/j.margeo.2004.05.029
Michard, A., Negro, F., Frizon de Lamotte, D., Saddiqi, O., 2007. Serpentinite slivers and metamorphism in the external Maghrebides: arguments for an intracontinental suture in the African paleomargin (Morocco, Algeria). Rev. Soc. Geológica Esp. 20, 173–185.
Palomeras, I., Carbonell, R., Flecha, I., Simancas, F., Ayarza, P., Matas, J., Martínez Poyatos, D., Azor, A., González Lodeiro, F., Pérez-Estaún, A., 2009. Nature of the lithosphere across the Variscan orogen of SW Iberia: Dense wide-angle seismic reflection data. J. Geophys. Res. 114. doi:10.1029/2007JB005050
Peron-Pinvidic, G., Manatschal, G., 2009. The final rifting evolution at deep magma-poor passive margins from Iberia-Newfoundland: a new point of view. Int. J. Earth Sci. 98, 1581–1597. doi:10.1007/s00531-008-0337-9
Ramos, A., Cascone, L., Olaiz, A., Fernández, O., Sánchez de la Muela, A., Hermoza, W., Arnaiz, A., Rocca, R., 2015. Crustal Structure of the Southern Portuguese Margin - Constraints from Potential Field Methods, paper presented at 77th EAGE Conference and Exhibition 2015. Presented at the 77th EAGE Conference and Exhibition 2015. doi:10.3997/2214-4609.201412974
Ramos, A., Fernández, O., Terrinha, P., Muñoz, J.A., 2017. Neogene to recent contraction and basin inversion along the Nubia-Iberia boundary in SW Iberia. Tectonics 36, 2016TC004262. doi:10.1002/2016TC004262
Ramos, A., Fernández, O., Terrinha, P., Muñoz, J.A., 2016. Extension and inversion structures in the Tethys–Atlantic linkage zone, Algarve Basin, Portugal. Int. J. Earth Sci. 105, 1663–1679. doi:10.1007/s00531-015-1280-1
Roeser, H.A., Steiner, C., Schreckenberger, B., Block, M., 2002. Structural development of the Jurassic Magnetic Quiet Zone off Morocco and identification of Middle Jurassic magnetic lineations. J. Geophys. Res. Solid Earth 107, EPM 1-1-EPM 1-23. doi:10.1029/2000JB000094
Roque, C., 2007. Tectonostratigrafia do cenozóico das margens continentais sul e sudoeaste portuguesas: um modelo de correlação sismostratigráfica. PhD Thesis, 310 pp. Universidade de Lisboa
Sallarès, V., Gailler, A., Gutscher, M.-A., Graindorge, D., Bartolomé, R., Gràcia, E., Díaz, J., Dañobeitia, J.J., Zitellini, N., 2011. Seismic evidence for the presence of Jurassic oceanic crust in the central Gulf of Cadiz (SW Iberian margin). Earth Planet. Sci. Lett. 311, 112–123. doi:10.1016/j.epsl.2011.09.003
Schettino, A., Turco, E., 2011. Tectonic history of the western Tethys since the Late Triassic. Geol. Soc. Am. Bull. 123, 89–105.
Seton, M., Müller, R.D., Zahirovic, S., Gaina, C., Torsvik, T., Shephard, G., Talsma, A., Gurnis, M., Turner, M., Maus, S., Chandler, M., 2012. Global continental and ocean basin reconstructions since 200 Ma. Earth-Sci. Rev. 113, 212–270. doi:10.1016/j.earscirev.2012.03.002
Sibuet, J.-C., Rouzo, S., Srivastava, S., 2012. Plate tectonic reconstructions and paleogeographic maps of the central and North Atlantic oceans. Can. J. Earth Sci. 49, 1395–1415. doi:10.1139/e2012-071
Smith, W.H., Sandwell, D.T., 1997. Global sea floor topography from satellite altimetry and ship depth soundings. Science 277, 1956–1962.
Spakman, W., Wortel, R., 2004. A Tomographic View on Western Mediterranean Geodynamics, in: Cavazza, P.D.W., Roure, D.F., Spakman, P.W., Stampfli,

P.G.M., Ziegler, P.P.A. (Eds.), The TRANSMED Atlas. The Mediterranean Region from Crust to Mantle. Springer Berlin Heidelberg, pp. 31–52.
Stampfli, G.M., Borel, G.D., 2002. A plate tectonic model for the Paleozoic and Mesozoic constrained by dynamic plate boundaries and restored synthetic oceanic isochrons. Earth Planet. Sci. Lett. 196, 17–33.
Talwani, M., 1965. Computation with the help of a digital computer of magnetic anomalies caused by bodies of arbitrary shape. Geophysics 30, 797–817. doi:10.1190/1.1439654
Talwani, M., Worzel, J.L., Landisman, M., 1959. Rapid gravity computations for two-dimensional bodies with application to the Mendocino submarine fracture zone. J. Geophys. Res. 64, 49–59. doi:10.1029/JZ064i001p00049
Terrinha, P., 1998. Structural geology and tectonic evolution of the Algarve Basin, South Portugal. PhD Thesis, 430 pp, Imperial College, London
Terrinha, P., Matias, L., Vicente, J., Duarte, J., Luís, J., Pinheiro, L., Lourenço, N., Diez, S., Rosas, F., Magalhães, V., Valadares, V., Zitellini, N., Roque, C., Víctor, L.M., 2009. Morphotectonics and strain partitioning at the Iberia–Africa plate boundary from multibeam and seismic reflection data. Mar. Geol. 267, 156–174. doi:10.1016/j.margeo.2009.09.012
Terrinha, P., Ribeiro, C., Kullberg, J.C., Lopes, C., Rocha, R., Ribeiro, A., 2002. Compressive episodes and faunal isolation during rifting, Southwest Iberia. J. Geol. 110, 101–113.
TGS, 2005. PD00: non-exclusive 2D Survey, TGS online data zone. (http://www.tgs.com/TGS/specsheets/PD-00_Spec.pdf).
Thiebot, E., Gutscher, M.-A., 2006. The Gibraltar Arc seismogenic zone (part 1): Constraints on a shallow east dipping fault plane source for the 1755 Lisbon earthquake provided by seismic data, gravity and thermal modeling. Tectonophysics 426, 135–152. doi:10.1016/j.tecto.2006.02.024
Torelli, L., Sartori, R., Zitellini, N., 1997. The giant chaotic body in the Atlantic Ocean off Gibraltar: new results from a deep seismic reflection survey. Mar. Pet. Geol. 14, 125–138. doi:10.1016/S0264-8172(96)00060-8
Torne, M., Fernàndez, M., Vergés, J., Ayala, C., Salas, M.C., Jimenez-Munt, I., Buffett, G.G., Díaz, J., 2015. Crust and mantle lithospheric structure of the Iberian Peninsula deduced from potential field modeling and thermal analysis. Tectonophysics 663, 419–433. doi:10.1016/j.tecto.2015.06.003
Tortella, D., Torne, M., Pérez-Estaún, A., 1997. Geodynamic evolution of the eastern segment of the Azores-Gibraltar zone: the Gorringe Bank and the Gulf of Cadiz region. Mar. Geophys. Res. 19, 211–230.
Tugend, J., Manatschal, G., Kusznir, N.J., Masini, E., Mohn, G., Thinon, I., 2014. Formation and deformation of hyperextended rift systems: Insights from rift domain mapping in the Bay of Biscay-Pyrenees. Tectonics 33, 1239–1276. doi:10.1002/2014TC003529
van Hinsbergen, D.J.J., Vissers, R.L.M., Spakman, W., 2014. Origin and consequences of western Mediterranean subduction, rollback, and slab segmentation. Tectonics 33, 393–419. doi:10.1002/2013TC003349
Vegas, R., Medialdea, T., Muñoz García, M., Díaz del Río, V., Somoza, L., 2004. Nature and tectonic setting of the Guadalquivier Bank (Gulf of Cadiz, SW Iberian Peninsula). Rev. Soc. Geológica Esp. 17, 49–60.

Vera, J.A., Molina, J.M., Aguado, R., 2004. Calcarenitas de Microcodium (Formación Majalcorón, Paleoceno, Subbético): descripción, bioestratigrafía y significado en el Terciario de la Cordillera Bética. Bol. Geológico Min. Esp. 115, 453–468.

Vergés, J., Fernàndez, M., 2012. Tethys–Atlantic interaction along the Iberia–Africa plate boundary: The Betic–Rif orogenic system. Tectonophysics 579, 144–172. doi:10.1016/j.tecto.2012.08.032

Wessel, P., Smith, W.H.F., 1998. New, improved version of generic mapping tools released. Eos Trans. Am. Geophys. Union 79, 579–579. doi:10.1029/98EO00426

Zeyen, H., Ayarza, P., Fernàndez, M., Rimi, A., 2005. Lithospheric structure under the western African-European plate boundary: A transect across the Atlas Mountains and the Gulf of Cadiz. Tectonics 24, TC2001. doi:10.1029/2004TC001639

Zitellini, N., Gràcia, E., Matias, L., Terrinha, P., Abreu, M.A., DeAlteriis, G., Henriet, J.P., Dañobeitia, J.J., Masson, D.G., Mulder, T., 2009. The quest for the Africa–Eurasia plate boundary west of the Strait of Gibraltar. Earth Planet. Sci. Lett. 280, 13–50. doi:10.1016/j.epsl.2008.12.005

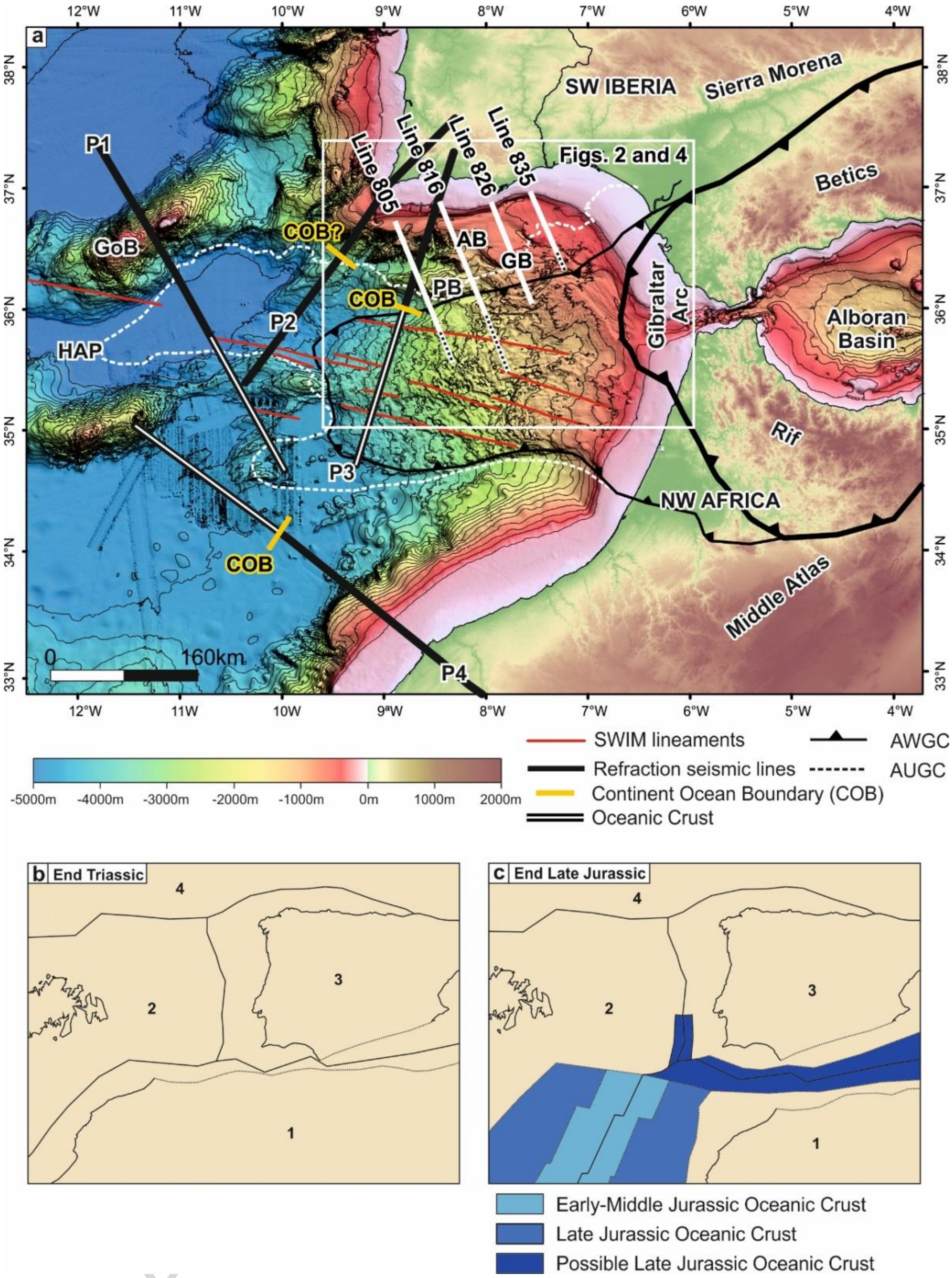

Fig. 1. a) Location of the study area. Traces of refraction seismic profiles acquired between SW Iberia and NW Africa are from Martínez-Loriente et al. (2014) (P1); González et al. (1996) (P2); Sallarès et al. (2011) (P3); and Contrucci et al. (2004) (P4). The location of the continent-ocean boundary (COB) defined on these lines is shown. The reflection seismic lines interpreted in this work are represented by white lines, while their prolongation to the SE for gravimetric modeling is marked with black dotted lines.

AB: Algarve Basin; AUGC: Allochthonous Unit of Gulf of Cadiz; AWGC: Accretionary Wedge of Gulf of Cadiz; GB: Guadalquivir Bank; GoB: Gorringe Bank; HAP: Horseshoe Abyssal Plain; PB: Portimão Bank. SWIM faults come from Zitellini et al. (2009). Bathymetry is taken from the General Bathymetric Chart of Oceans (GEBCO) digital atlas (IOC et al., 2003) and topography from European Environment Agency (EEA). (b) Plate reconstruction at end of Triassic (203 Ma) and (c) at end of Jurassic times (151 Ma) modified after Schettino and Turco (2011), Seton et al. (2012), and Sibuet et al. (2012). 1: NW Nubia, 2: North America, 3: Iberia, 4: Armorica-Greenland.

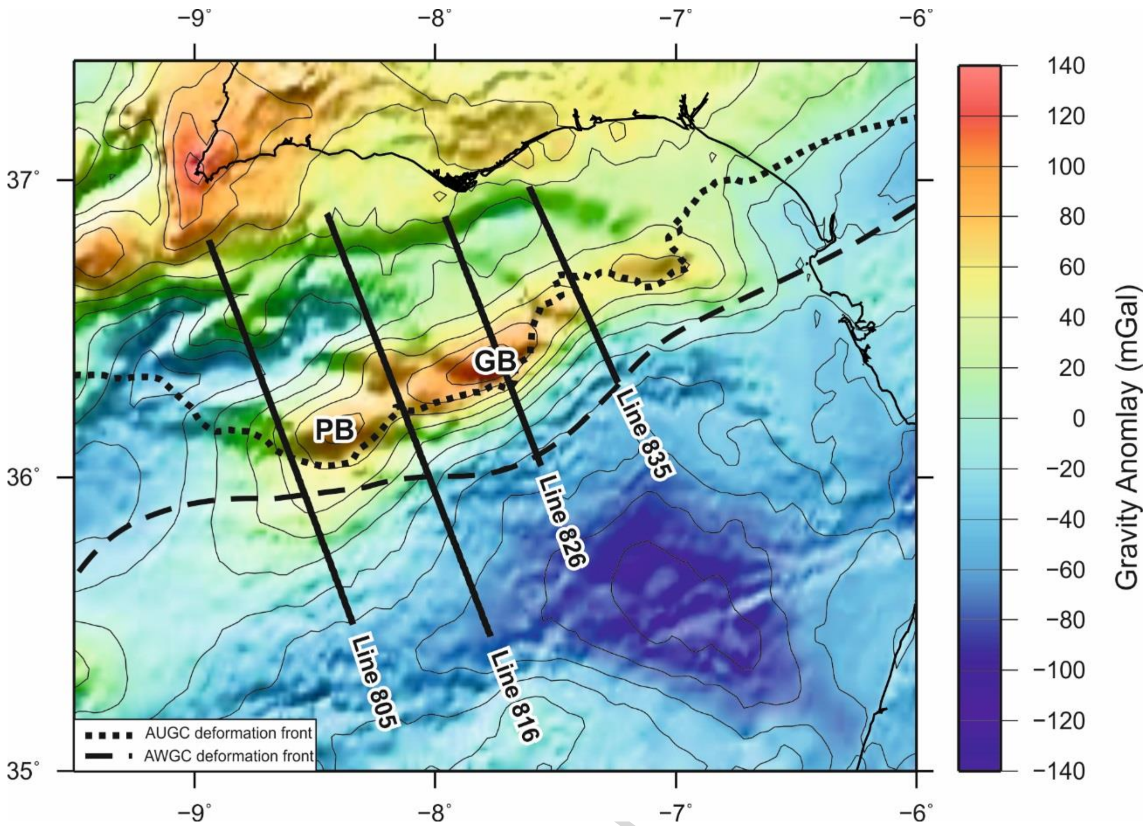

Fig. 2. Map of free-air gravity anomaly offshore and Bouguer anomaly onshore. Black lines show the location of the 2D gravimetric profiles presented in this study. Note the ENE-WSW trending positive gravity anomaly located offshore (> 40 mGal), and the negative gravity anomaly (<-60 mGal) to the SE. GB: Guadalquivir Bank; PB: Portimão Bank.

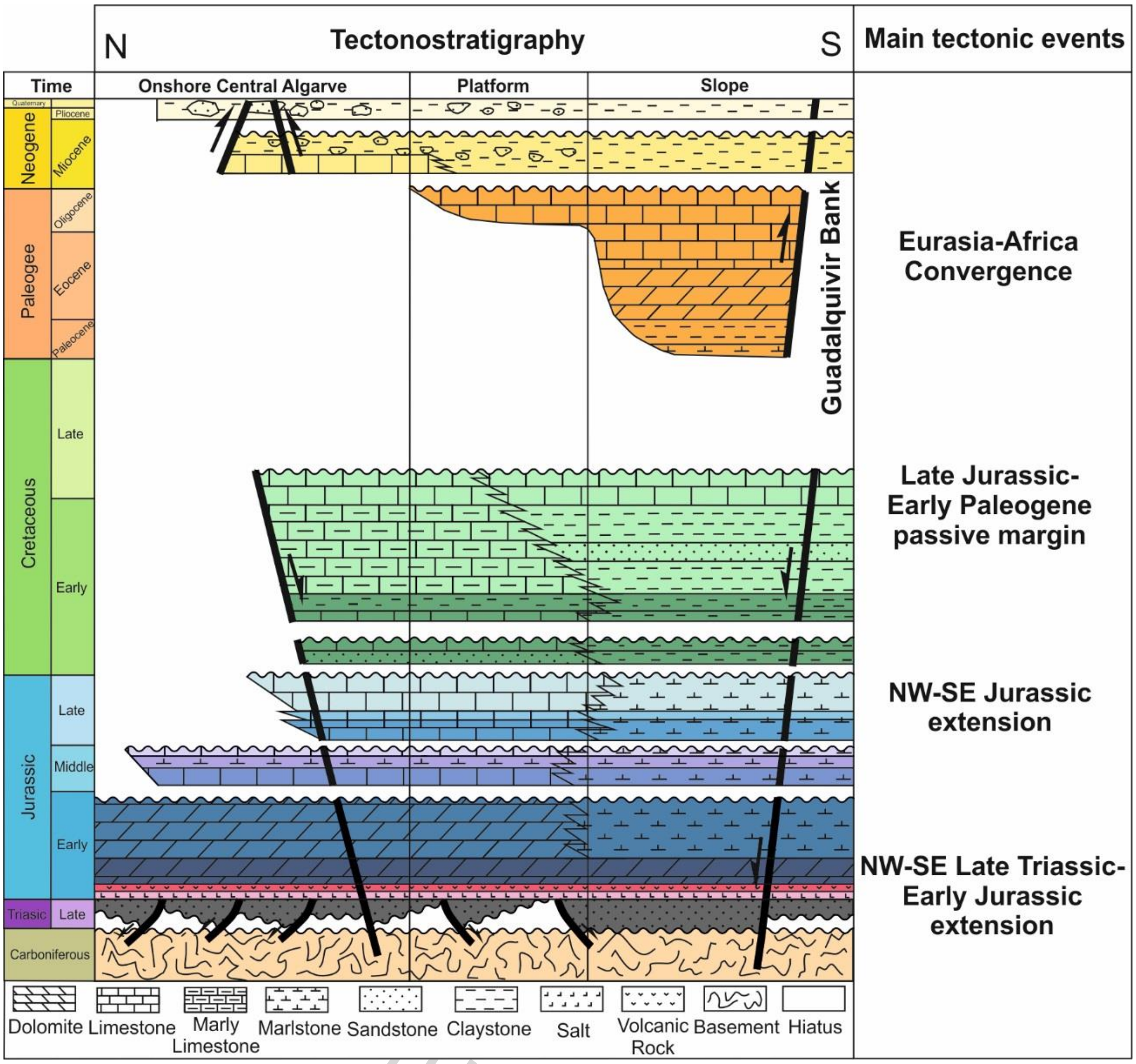

Fig. 3. Tectono-sedimentary diagram of the Algarve Basin showing the main stratigraphic units and tectonic events. Modified from Ramos et al. (2016).

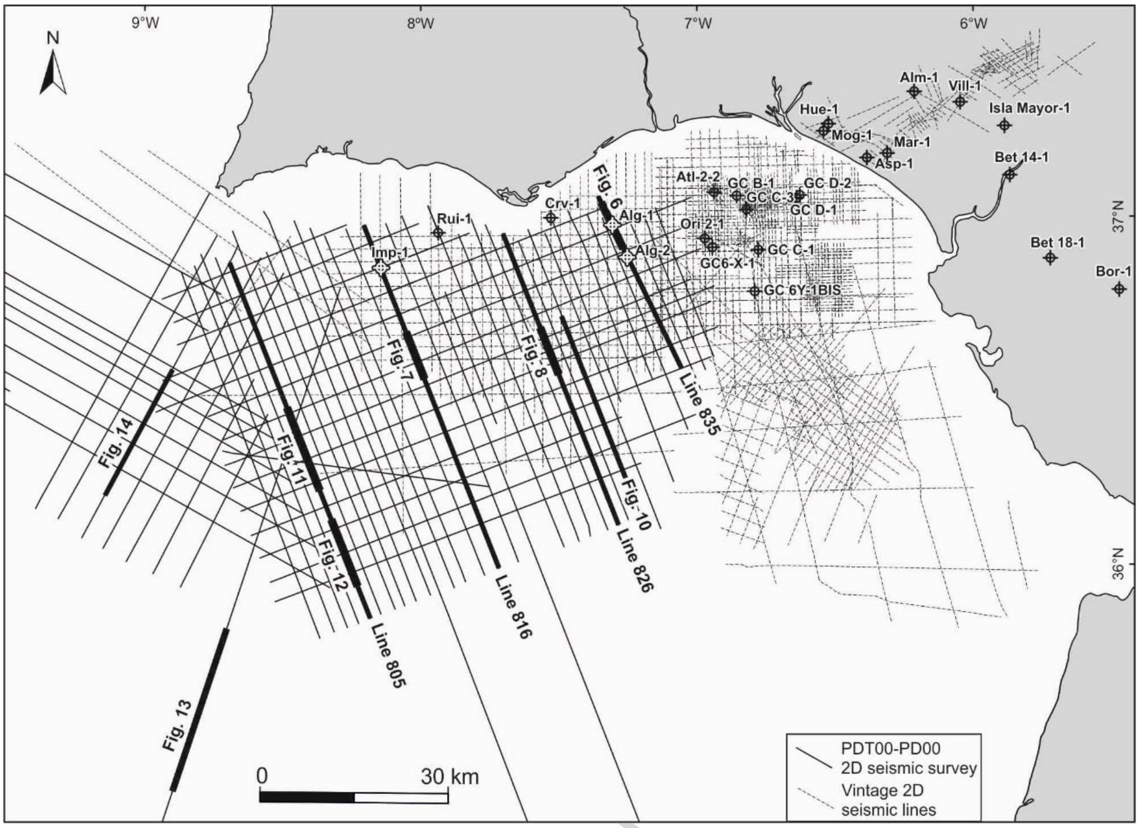

Fig. 4. Data in the Gulf of Cadiz used in this study. The most representative and complete wells shown in this figure are: Alg-1: Algarve-1; Alg-2; Algarve-2; Alm-1: Almonte-1; Asp-1: Asperillo-1; Atl-2-2: Atlantida-2-2; Bet 14-1: Betica 14-1; Bet 18-1: Betica 18-1; Bor-1: Bornos-1; Crv-1: Corvina-1; GC6-X-1; Gulf of Cadiz 6-X-1; GC B-1: Gulf of Cadiz B-1; GC B-2: Gulf of Cadiz B-2; GB D-1: Gulf of Cadiz D-2; GB D-2: Gulf of Cadiz D-2; GB 6Y-1Bis: Gulf of Cadiz 6Y-1Bis; Hue-1: Huelva-1; Imp-1: Imperador-1; Mar-1: Marismas-1; Mog-1: Moguer-1; Ori 2-1: Orion 2-1; Rui-1: Ruivo-1.

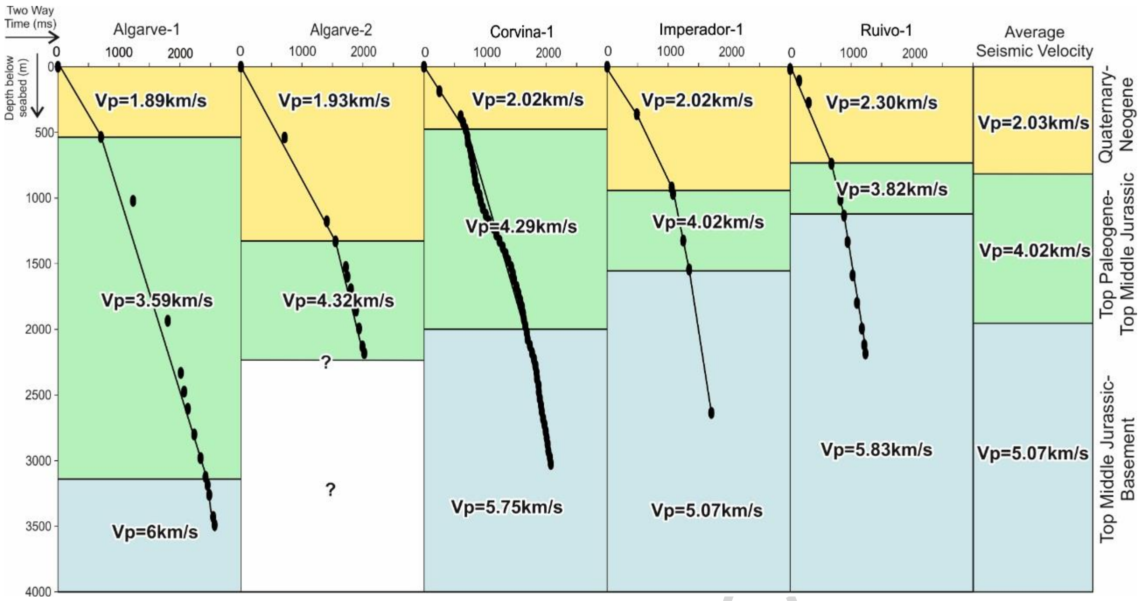

Fig. 5. Checkshot data from the 5 wells in the Portuguese Algarve Basin. See Fig. 4 for location. The time-depth relationships from the 5 wells have been used to define 3 velocity intervals: Neogene-Quaternary (yellow), top Paleogene to top Middle Jurassic (green) and top Middle Jurassic to top of Basement (blue). Data courtesy of Repsol.

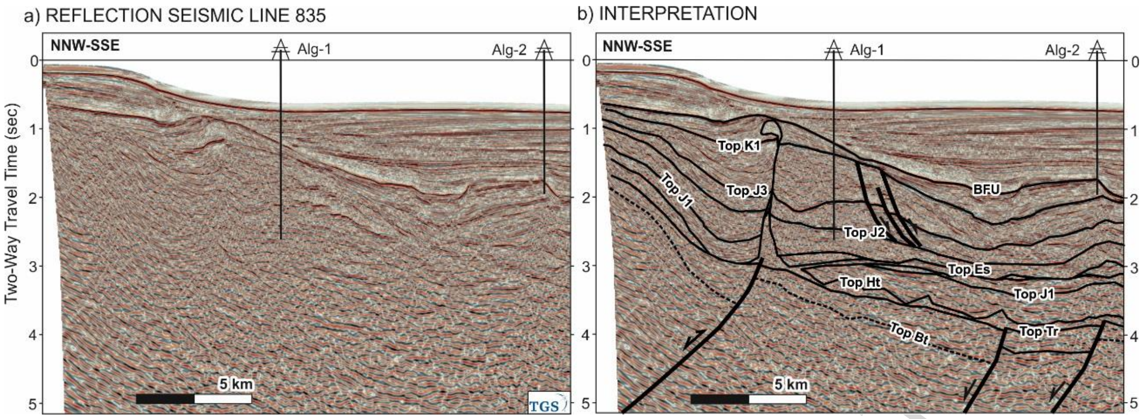

Fig. 6. Portion of seismic line 835 across wells Algarve-1 and Algarve-2 in time (a), and seismic interpretation (b). BFU: base foredeep unconformity; K1: Lower Cretaceous; J3: Upper Jurassic; J2: Middle Jurassic; J1: Upper Jurassic; Tr: Triassic; Ht: Hettangian. The allochthonous Esperança salt unit (Matias et al., 2011) is also identified (Es). See Fig. 4 for location.

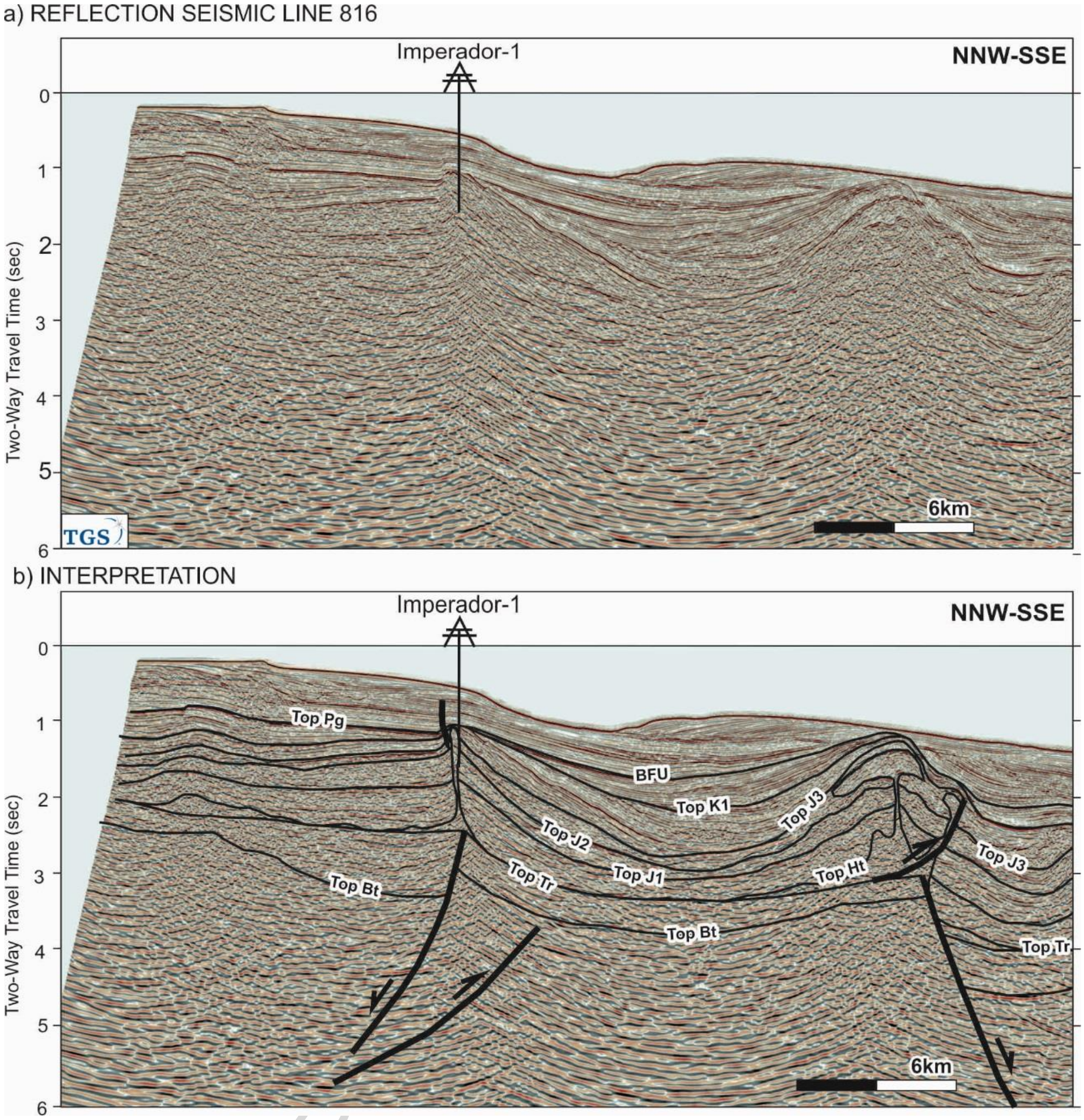

Fig. 7. Portion of seismic line 816 across the well Imperador-1, in time (a) and seismic interpretation (b). See Fig 4 for location and Fig. 6 for acronyms. Data courtesy of TGS.

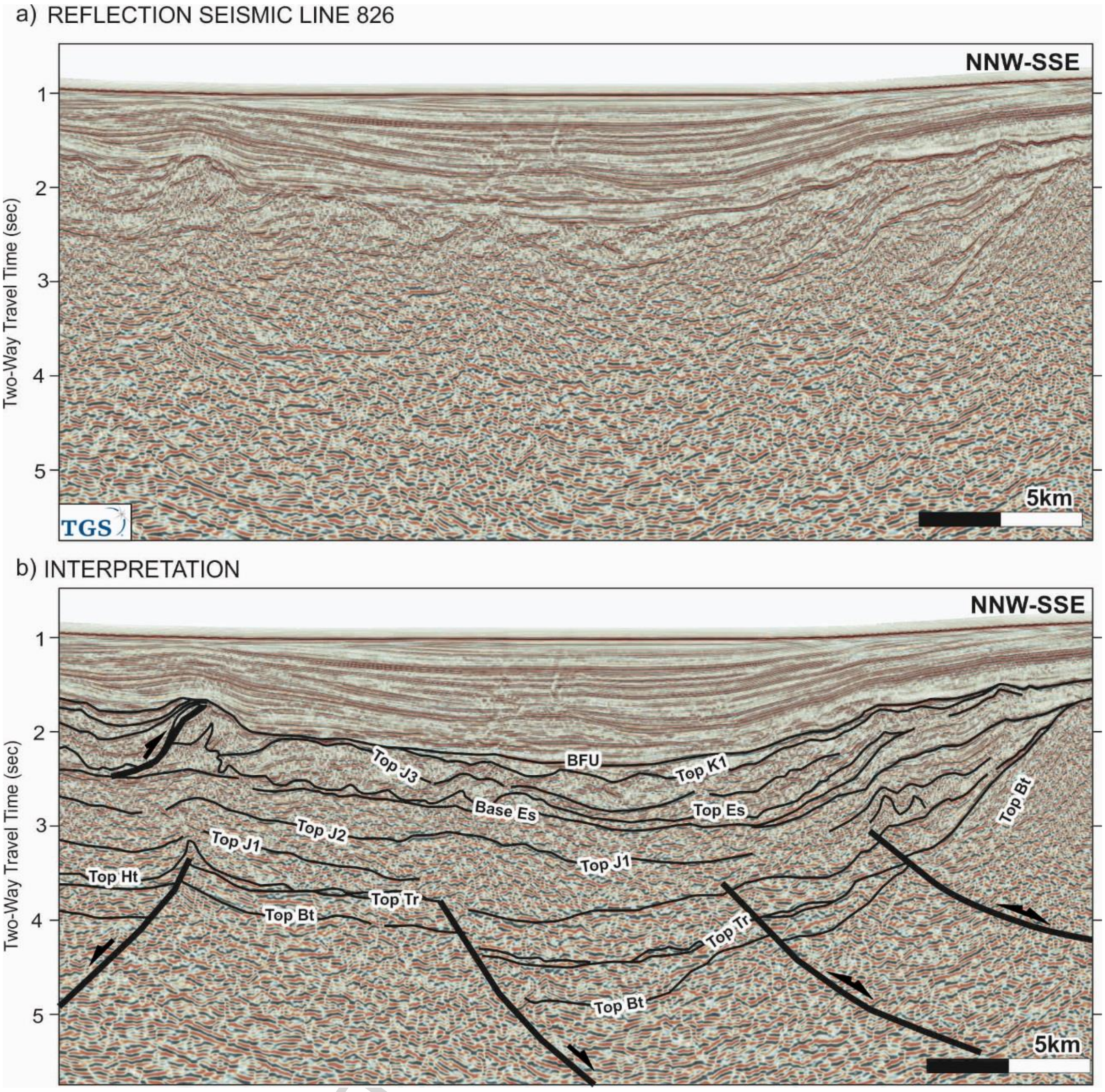

Fig. 8. Portion of seismic line 826 in the central part of the Algarve Basin, in time (a) and seismic interpretation (b) in the central part of the basin, north of Guadalquivir Bank. Es: Esperança Salt. See Fig 4 for location and Fig. 8 for acronyms. Data courtesy of TGS.

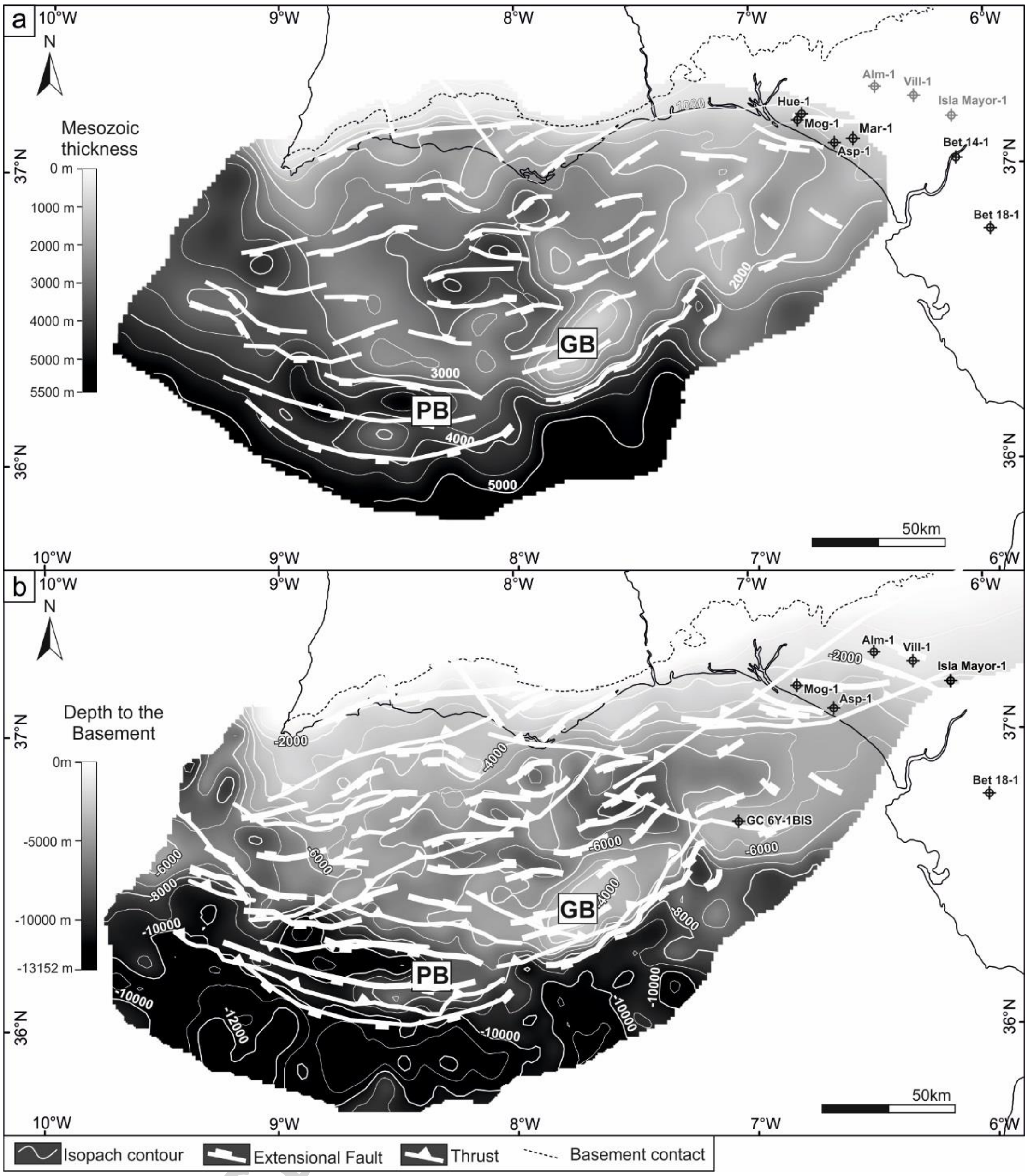

Fig. 9. (a) Vertical thickness of Mesozoic (Triassic to Lower Cretaceous) in the SW Iberian margin, with the main Mesozoic extensional faults overlain. Wells on the onshore that encounter Mesozoic sediments are shown in black. Wells that encountered no autochthonous Mesozoic are shown in grey. The Betica 14-1 was finalized upon reaching the top of the autochthonous Mesozoic (Upper Jurassic) and no reliable thickness value can be derived. The Betica 18-1 well drilled 2700m of Mesozoic (Upper and Lower Cretaceous, Jurassic and Triassic). (b) Structural map of the top of basement, affected by Mesozoic extensional faults and Cenozoic thrusts (thrusts from Ramos et al., submitted). Wells reaching the

basement are represented in the figure. The Betica 18-1 well encountered the basement at 4280m bsl, but has not been incorporated in the map due to lack of constraint from MCS profiles. See Fig. 4 for complete well names and location of MCS profiles.

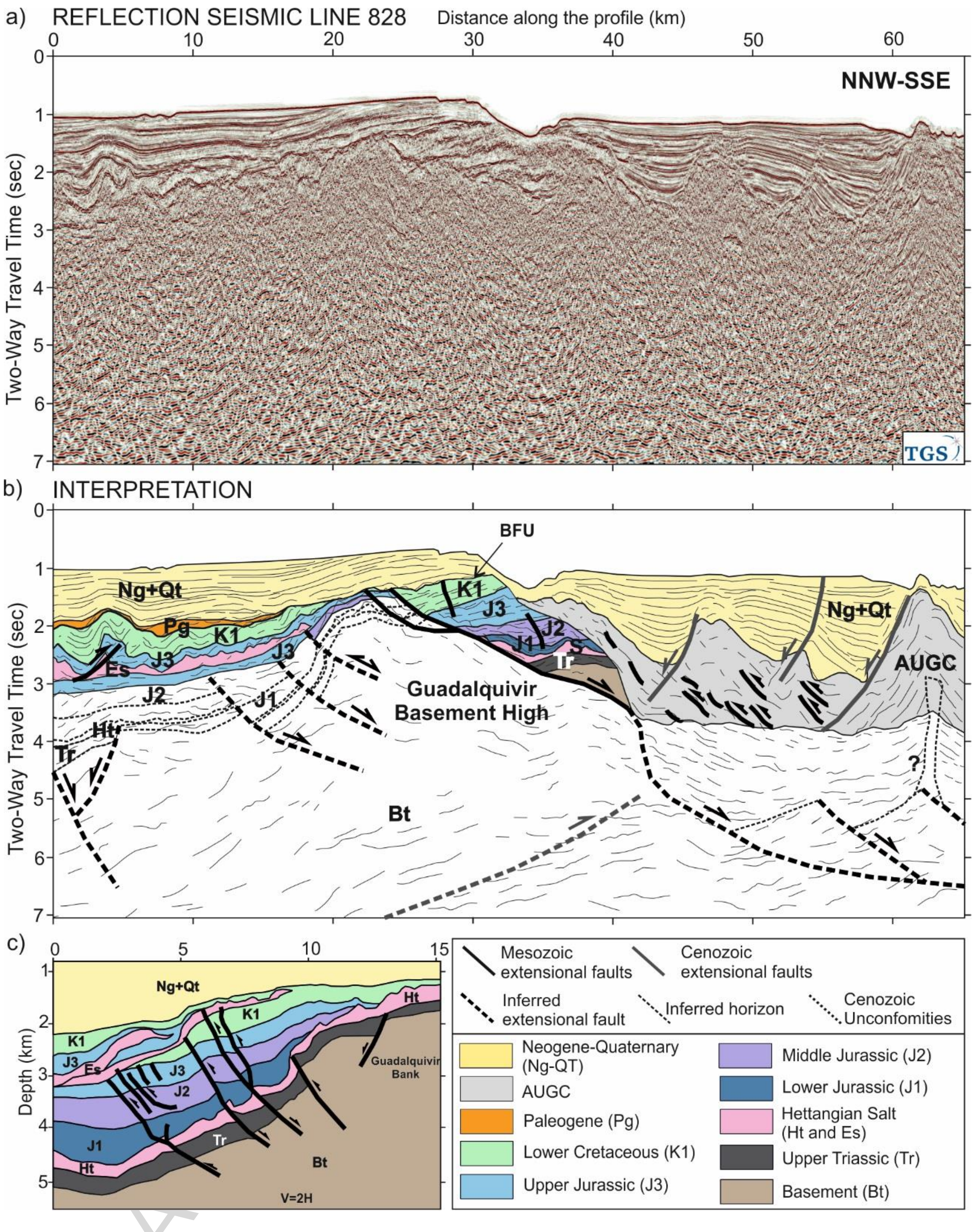

Fig. 10. Portion of seismic line 828 across the Guadalquivir Bank in time (a) and seismic interpretation (b). The interpretation below 3-4 seconds of TWT is inferred due to the poor deep seismic quality. Interpretation of the northern flank of the Guadalquivir Bank is based on the interpretation performed on 3D seismic (c) of the same structure slightly along strike by (Ramos et al., submitted). See Fig. 4 for location. Data courtesy of TGS.

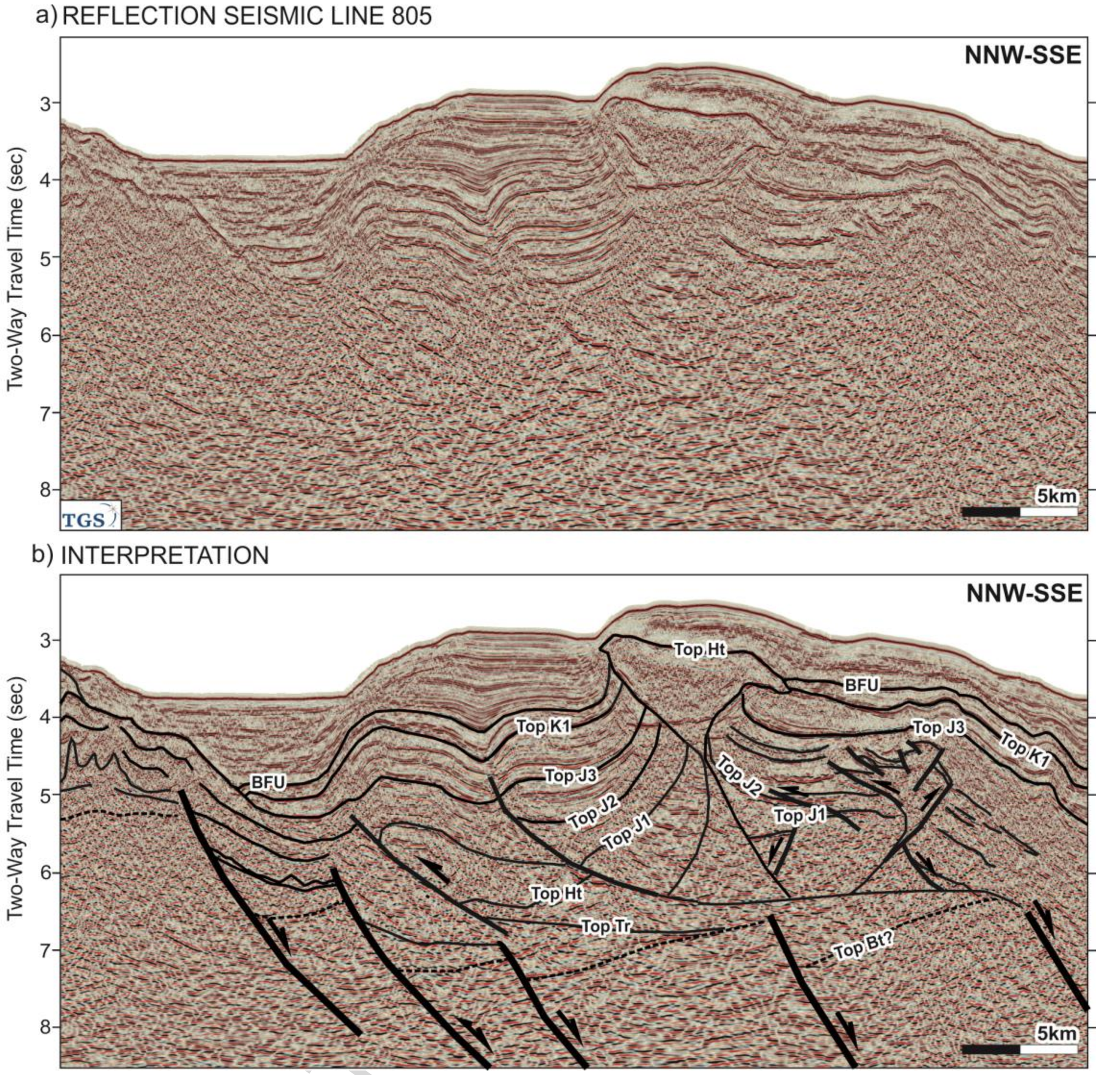

Fig. 11. Portion of seismic line 805 across the Portimão Bank in time (a) and seismic interpretation (b). The Portimão Bank is imaged as an inverted Mesozoic graben. See Fig 4 for location and Fig. 8 for acronyms. Data courtesy of TGS.

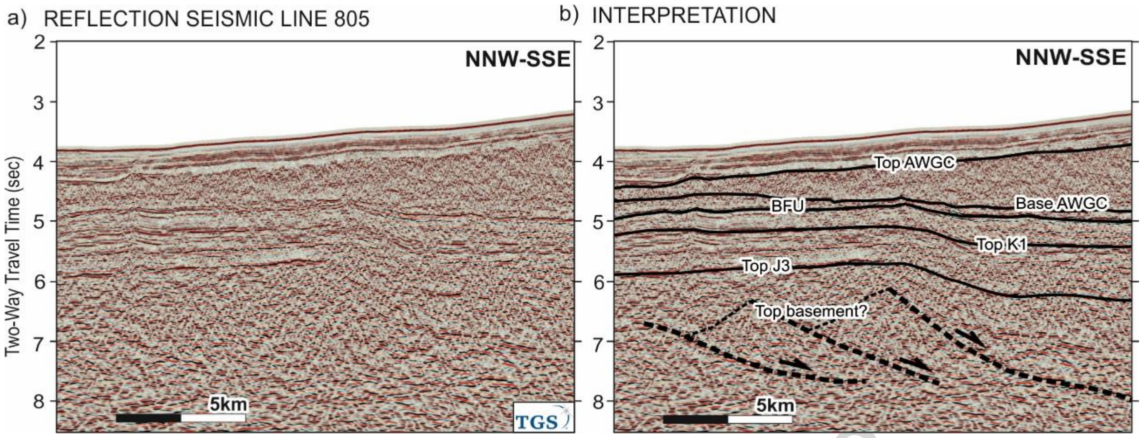

Fig. 12. Portion of seismic line 805 south of the Portimão Bank, across a distal portion of the AWGC, in time (a) and seismic interpretation (b). Note that Mesozoic units are visible under the AWGC and the top of the basement is imaged around 7 seconds of TWT. See Fig 4 for location and Fig. 8 for acronyms. Data courtesy of TGS.

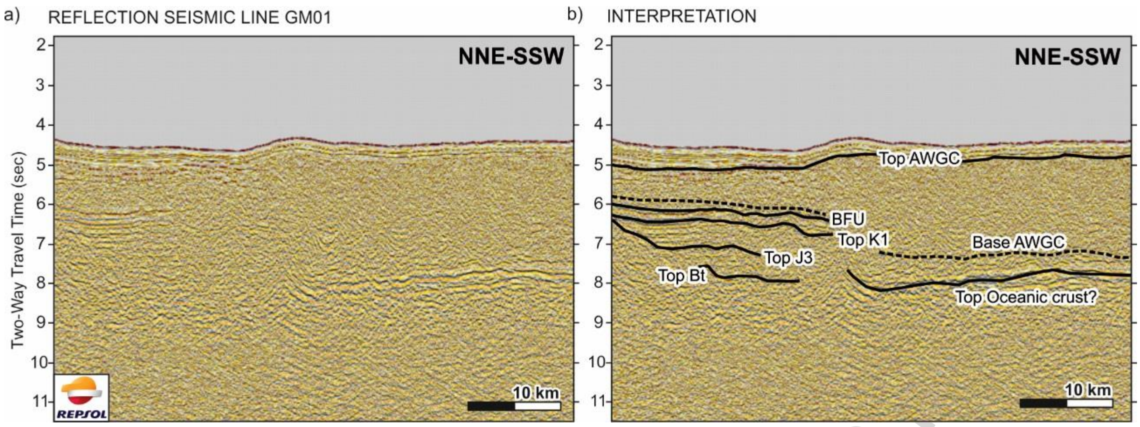

Fig. 13. Portion of a seismic profile GM01 across the outer Gulf of Cadiz in time (a) and seismic interpretation (b). Note the bright continuous reflectors under the AWGC interpreted to be the top of oceanic crust. See Fig. 4 for location. Data courtesy of Repsol.

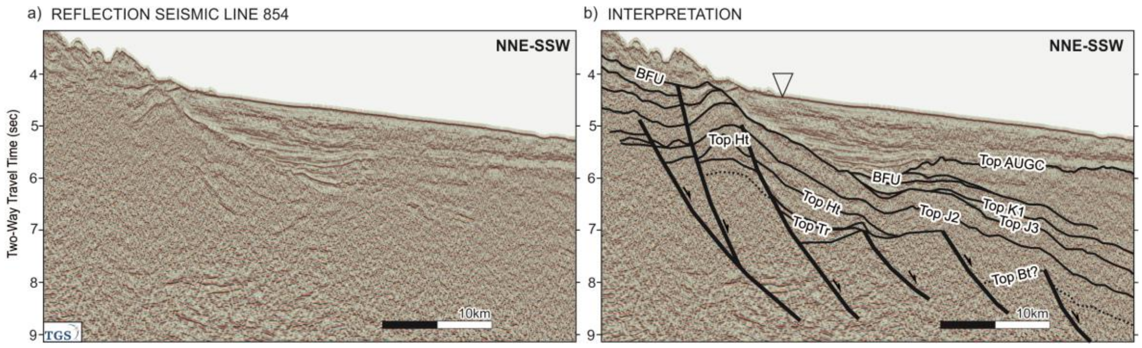

Fig. 14. Portion of reflection seismic profile 854 across the western portion of the margin (a) and the corresponding interpretation (b). The triangle on the seabed marks the location of the transfer discussed in Fig. 18. See Fig. 4 for location. Data courtesy of TGS.

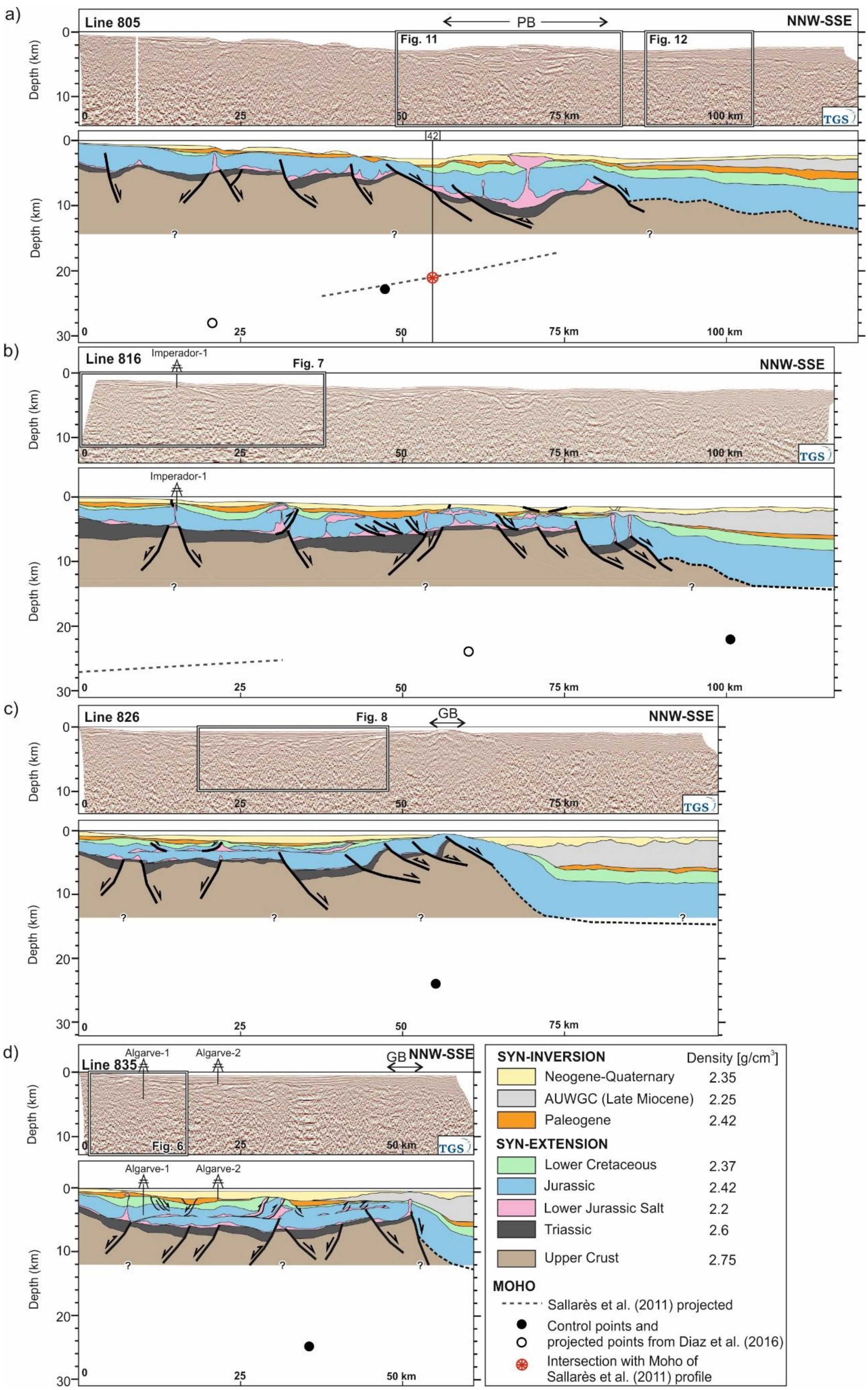
a)
Line 805
PB
NNW-SSE
Fig. 11
Fig. 12
Depth (km)
TGS
42
b)
Line 816
Imperador-1
Fig. 7
NNW-SSE
c)
Line 826
Fig. 8
GB
NNW-SSE
d)
Line 835
Algarve-1
Algarve-2
GB
NNW-SSE
Fig. 6
SYN-INVERSION
Density [g/cm3]
Neogene-Quaternary 2.35
AUWGC (Late Miocene) 2.25
Paleogene 2.42
SYN-EXTENSION
Lower Cretaceous 2.37
Jurassic 2.42
Lower Jurassic Salt 2.2
Triassic 2.6
Upper Crust 2.75
MOHO
Sallarès et al. (2011) projected
Control points and
projected points from Diaz et al. (2016)
Intersection with Moho of
Sallarès et al. (2011) profile

Fig. 15. Interpretation of depth converted seismic profiles through the Algarve Basin, shown from west (top) to east (bottom): a) Line 805; b) Line 816; c) Line 826; and d) Line 835. The control points on the depth of Moho from the compilation of Diaz et al. (2016) and the profile of Sallarès et al. (2011) are shown. Average interval densities are shown in the legend. GB: Guadalquivir Bank; PB: Portimão Bank. See Figs. 1a and 4 for location. Data courtesy of TGS.

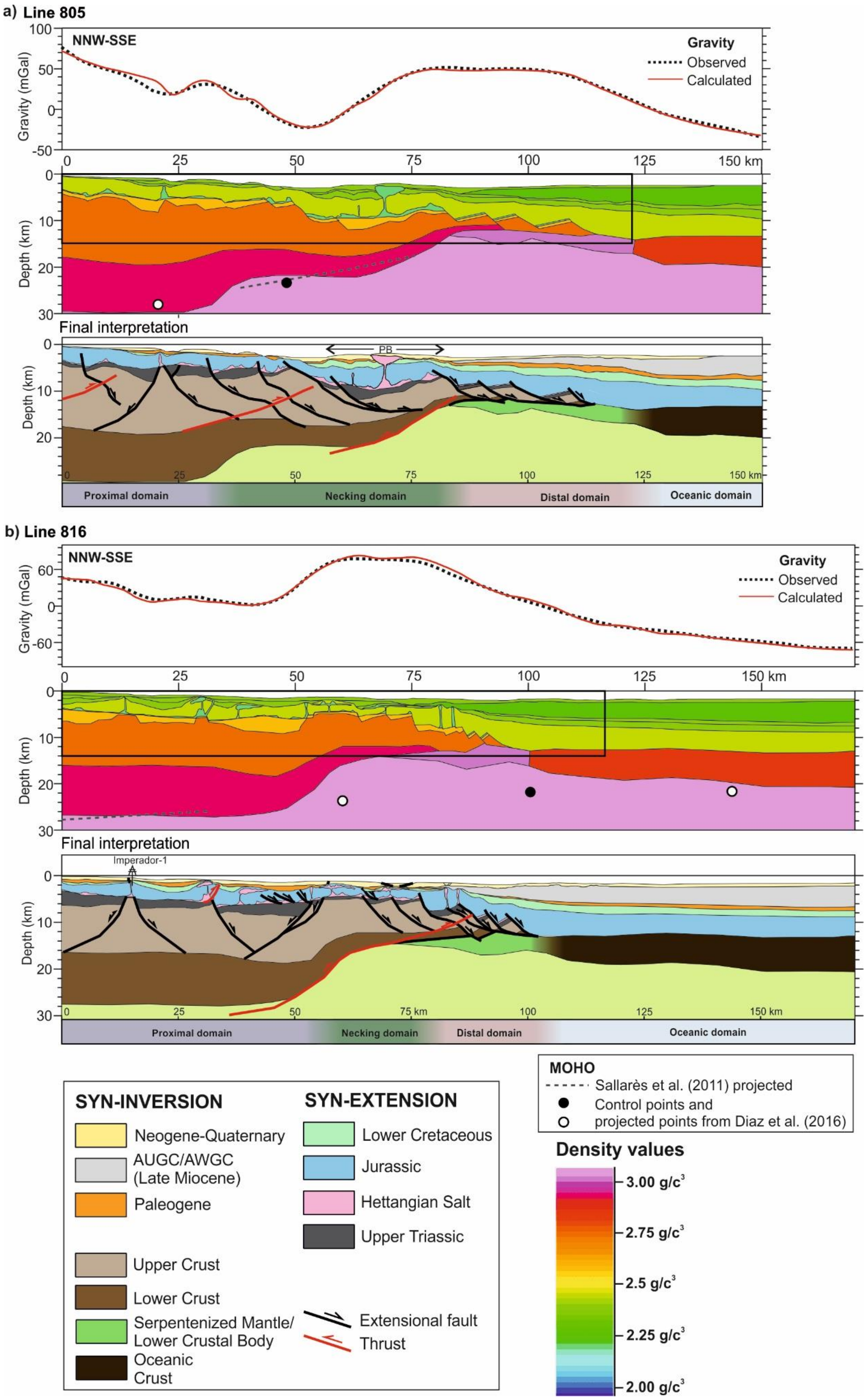
a) Line 805
NNW-SSE
Gravity
Observed
Calculated
Gravity (mGal)
Depth (km)
Final interpretation
PB
Proximal domain
Necking domain
Distal domain
Oceanic domain
b) Line 816
Imperador-1
SYN-INVERSION
Neogene-Quaternary
AUGC/AWGC (Late Miocene)
Paleogene
Upper Crust
Lower Crust
Serpentenized Mantle/ Lower Crustal Body
Oceanic Crust
SYN-EXTENSION
Lower Cretaceous
Jurassic
Hettangian Salt
Upper Triassic
Extensional fault
Thrust
MOHO
Sallarès et al. (2011) projected
Control points and
projected points from Diaz et al. (2016)
Density values
3.00 g/c3
2.75 g/c3
2.5 g/c3
2.25 g/c3
2.00 g/c3

Fig. 16. Composition of observed and forward modelled gravity, density model and final interpretation for profiles along lines 805 (a) and 816 (b). The geometry of the sedimentary layers, from Triassic to Quaternary, has been derived from the interpretation of MCS data (Fig. 15). Extent of the seismic profiles is represented by a black box on the density model. Densities used are also shown in the table on Fig. 15. The Moho from the profile of Sallarès et al. (2011) has been projected onto the density models over the pertinent segments. Points from the compilation by Diaz et al. (2016) lying on the modelled profiles (black) and projected from nearby locations (white) are also shown on the density model. On the final interpretation note the combination of Mesozoic extensional and Cenozoic contractional features (from Ramos et al., submitted). See text for a discussion of the defined crustal domains. PB: Portimão Bank. See Fig. 2 for location.

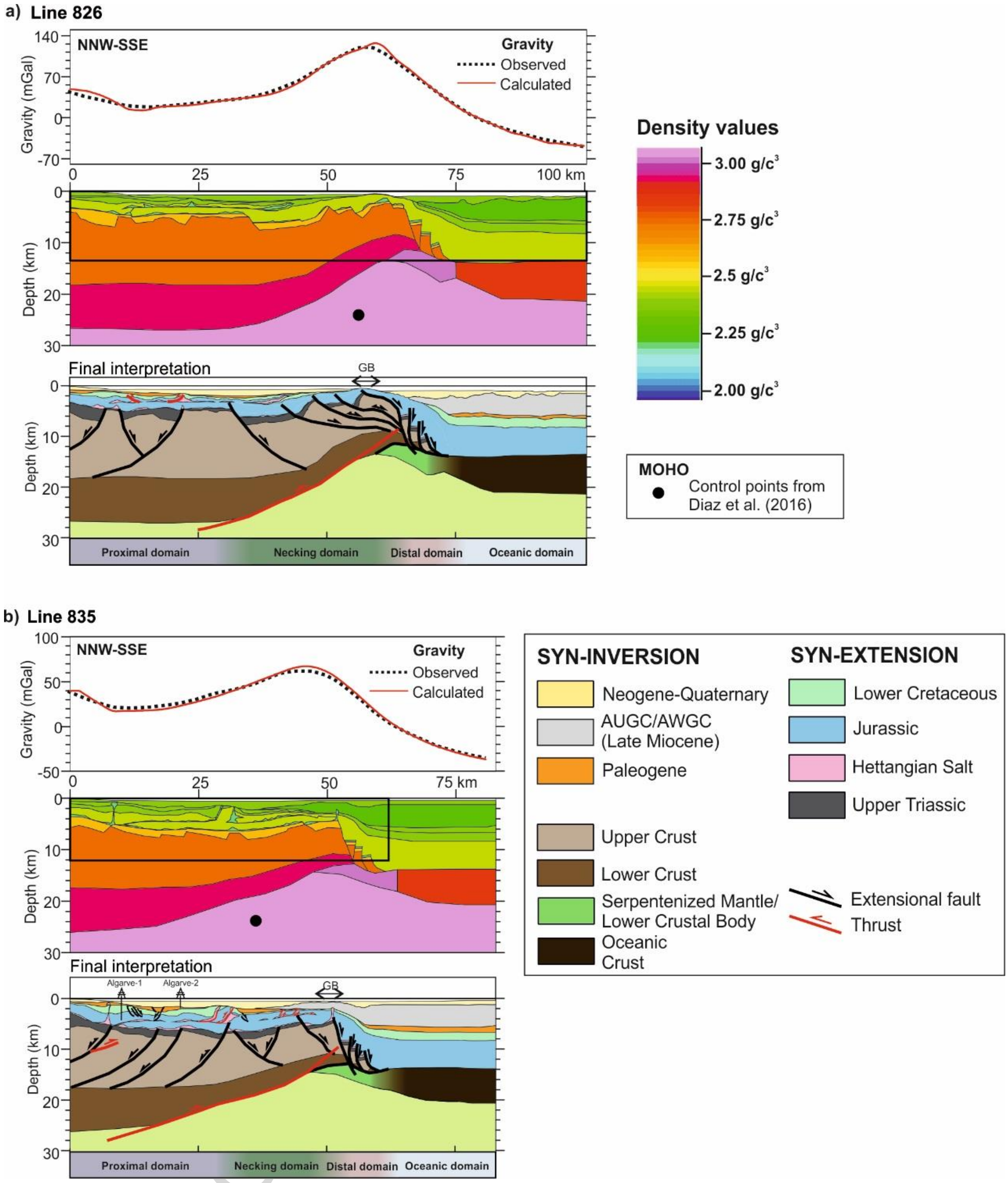

Fig. 17. Composition of observed and forward modelled gravity, density model and final interpretation for profiles along lines 826 (a) and 835 (b). The geometry of the sedimentary layers, from Triassic to Quaternary, has been derived from the interpretation of MCS data (Fig. 15). Extent of the seismic profiles is represented by a black box on the density model. Densities used are also shown in the table on Fig. 15. The Moho control points from Diaz et al. (2016) are shown on the density model. On the final interpretation note the combination of Mesozoic extensional and Cenozoic contractional features (from Ramos et al., submitted). The geometry on the southern end of the profiles is partly inferred from that

seen on the western profiles (Fig. 16). See text for a discussion of the defined crustal domains. GB: Guadalquivir Bank. See Fig. 2 for location.

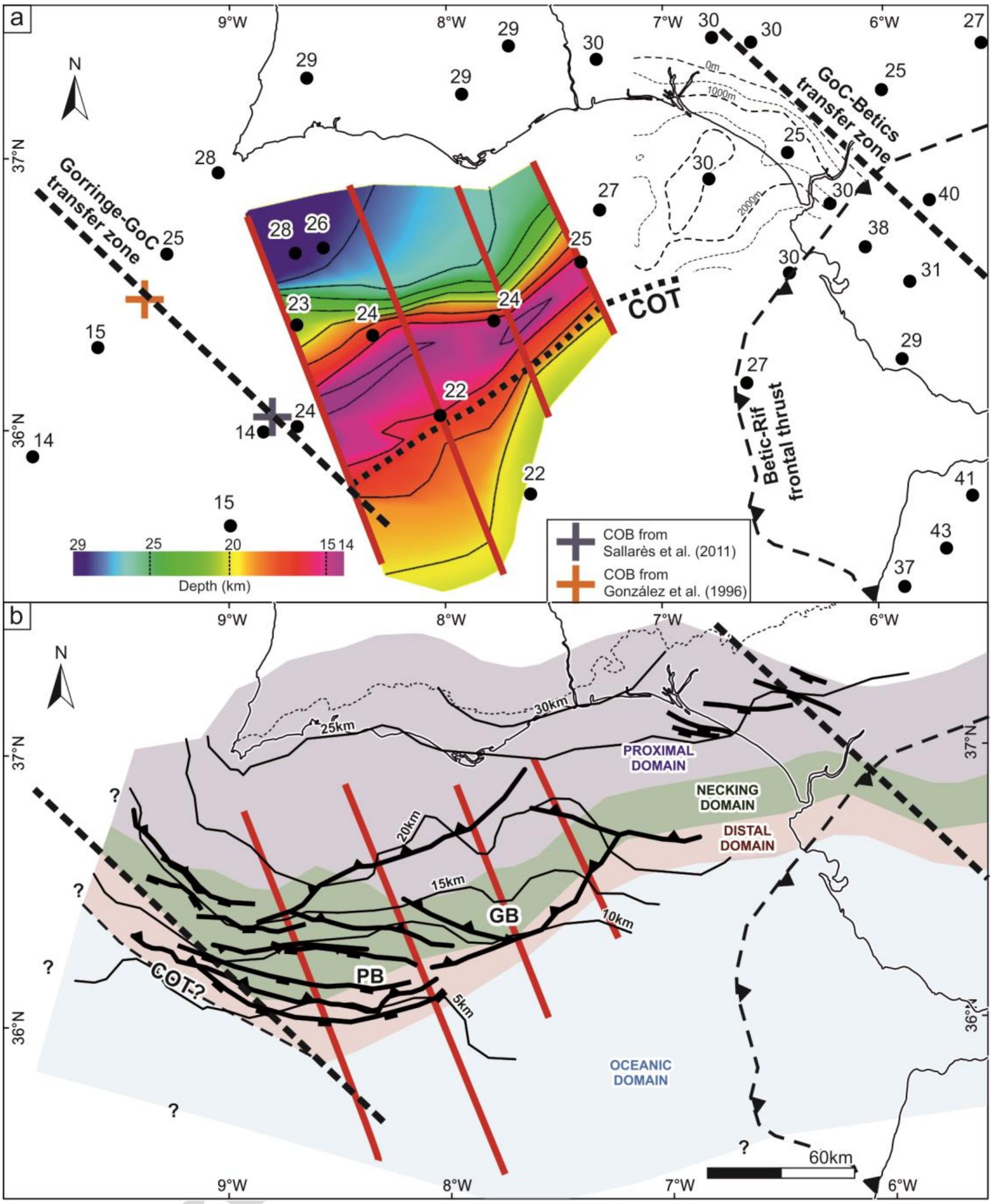

Fig. 18. a) Map of the base of the crust derived from seismic interpretation and gravimetric modeling. The COT (continent-ocean transition) derived from gravimetric modeling is shown by the bold dashed line. Points with numbers indicate the depth to the base of the crust from the compilation of Diaz et al. (2016). The western limit of the Gulf of Cadiz (GoC) segment of the margin is marked by the Gorringe-GoC transfer zone along the transition from continental to ocean domains defined by González et al., (1996) and Sallarès et al. (2011). The eastern limit of the margin segment is located along the GoC-Betic transfer zone, across which Mesozoic thickness drops (dashed contours indicate Mesozoic thickness in

this area from the map in Fig. 9a). b) Map of crustal thickness of SW Iberia with crustal domains (proximal, necking, and distal) defined through gravimetric modeling and from crustal thickness. Thrusts relevant to the discussion, mapped by Ramos et al. (submitted), and relevant extensional faults from Fig. 9a are superimposed.

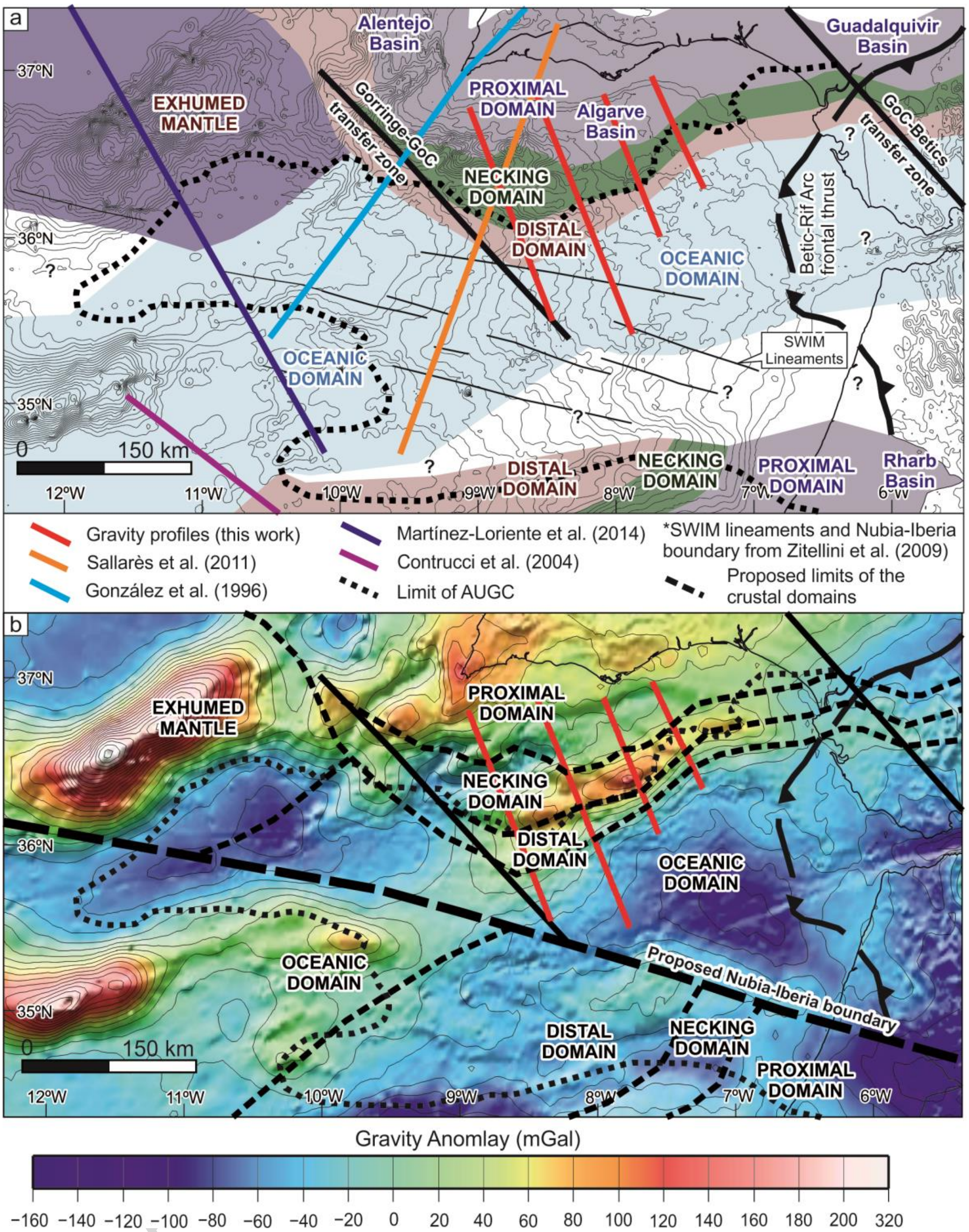

Fig. 19. a) Map of the main crustal domains of the Gulf of Cadiz and surrounding areas. Bathymetry is shown in the background (contours every 200m). The location of bibliographic profiles is shown. The domains defined for the Morocco margin are derived by projecting the domains defined by Contrucci et al. (2004). b) Map of the free-air gravity anomaly map (offshore) and Bouguer gravity anomaly (onshore)

of the SW Iberian margin with the crustal domain distribution based on integrated regional 2D seismic data and gravimetric modeling. Thin dashed black lines: crustal domain boundaries.

Highlights

- SW Iberian crust records a combination of Mesozoic extension and Cenozoic inversion
- Crustal domains resulting from extension are mapped for the SW Iberian margin
- SW Iberia is a segment of the transform margin connecting Tethys and Atlantic
- Inversion of SW Iberia concentrates in the most distal domains of the margin

ACCEPTED MANUSCRIPT